Disturbance Rejection MPC Framework for Input-Affine Nonlinear Systems

Huahui Xie, Li Dai, Yuchen Lu, and Yuanqing Xia, *Senior Member, IEEE*

***Abstract*—This article proposes a novel disturbance rejection model predictive control (DRMPC) framework to improve the robustness of model predictive control (MPC) for a broad class of input-affine nonlinear systems with constraints and state-dependent disturbances. The proposed controller includes two parts—a disturbance compensation input and an optimal MPC control input. The former one is designed to compensate for the matched disturbance actively. This is made possible via a disturbance observer that estimates the disturbance and by adopting a space decomposition method. The residual disturbance is then handled in the MPC optimization problem by appropriate tightening of the constraints and designing the terminal constraint. Under reasonable assumptions, recursive feasibility and regional input-to-state practical stability (regional ISpS) of the closed-loop system are shown. Furthermore, we extend the DRMPC framework toward the tracking problem and apply it to a nonholonomic mobile robot. The performance of the proposed approach is demonstrated by a numerical example of the nonholonomic mobile robot.**

***Index Terms*—Disturbance observer, input-affine nonlinear systems, model predictive control (MPC), robust control.**

I. Introduction

MODEL predictive control (MPC) [1], [2], also known as receding horizon control (RHC), is an outstanding optimization-based control technique with a great development prospect. Nevertheless, the strong theoretical properties, even the stability of the system, may not be ensured when suffering external disturbances. In the field of MPC, it remains an urgent need and ongoing challenge to alleviating the negative effect of disturbances.

An intuitive idea to reject disturbances is to take robustness into account for MPC design. The so-called robust MPC ensures a desirable control performance in the worst case of disturbances. For example, typically, min–max MPC [3]–[6] minimizes the effect of disturbances by considering and embedding the worse-case realization of disturbances into the MPC optimization problem. However, min–max MPC is often difficult to implement on account of its prohibitive computational burden. Therefore, to overcome this difficulty and obtain a computationally tractable MPC formulation, the inherent robustness of nominal MPC is introduced by removing uncertainty in the optimization problem. Correspondingly, in the nominal optimal control problem, the state and input constraints need to be tightened in case the practical physical constraints are violated in the presence of uncertainty. An impressive example is tube-based MPC originated from the seminal papers [7], [8]. In the tube-based MPC [9], a hierarchical control strategy is adopted, which includes an optimal controller to achieve a desirable control performance of the nominal system and an auxiliary controller to restrain the difference between the nominal system and the real perturbed system. However, for nonlinear systems, the existing open-loop optimization approaches based on nominal systems are still quite susceptive to external disturbances.

Disturbance observer-based technique is a promising method to improve the robustness of MPC by estimating and compensating disturbances simultaneously. The resulting bounds on the disturbance estimation error and the disturbance estimation are taken advantage of in the design of robust MPC, referred to as disturbance observer-based MPC. The similar idea has been adopted in some works by integrating disturbance observers into other advanced control strategies, such as neural network controller [10], sliding mode controller [11] and $\mathscr{H}_\infty$ controller [12]. In contrast to the prosperity in other advanced control methods, there have been relatively limited research results on disturbance observer-based MPC. By utilizing the disturbance compensation, the authors of [13] investigate the single-input and single-output affine nonlinear system and its linear version is provided in [14]. In [15], a disturbance observer-based predictive torque control approach is presented for induction motor systems. The disturbance observer technique is adopted to reject the influence of parameter uncertainties, which improves speed and torque responses and achieves better robustness. For these papers, the disturbance assumption is relatively strict and the variation of disturbance is assumed to vanish asymptotically. The assumptions on disturbances are relaxed in [16]–[23]. In [16] and [17], for three-phase inverters, the disturbance observer within the MPC framework is designed to both simplify the prediction model and improve the robustness against model uncertainties. In [18], a deadbeat MPC controller with stator current and disturbance observer is presented. The effect of disturbance

Manuscript received 11 May 2021; revised 27 September 2021; accepted 19 November 2021. Date of publication 7 December 2021; date of current version 5 December 2022. This work was supported in part by the National Natural Science Foundation of China under Grant 61836001, Grant 61803033, Grant 61720106010, Grant 62122014, and Grant 62173036. Recommended by Associate Editor Eric C. Kerrigan. *(Corresponding authors: Yuanqing Xia; Li Dai.)*

The authors are with the School of Automation, Beijing Institute of Technology, Beijing 100081, China (e-mail: xiehuahui19@gmail.com; li.dai@bit.edu.cn; luyuchen@bit.edu.cn; xia_yuanqing@bit.edu.cn).

Color versions of one or more figures in this article are available at https://doi.org/10.1109/TAC.2021.3133376.

Digital Object Identifier 10.1109/TAC.2021.3133376

mismatch is analyzed and considered in the observer design. A more reasonable composition of disturbance observer with MPC is proposed in offset-free control for linear systems [19], [20] and for nonlinear systems [21], [22]. Inspired by these works, the authors of [23] further consider input constraints and the input-to-state stability is proved by introducing an artificial state constraint. However, these works do not guarantee recursive feasibility and stability under physical constraints (including input and state constraints). In addition, with the mature of constrained MPC implementation, there is a lack of a unified framework to introduce the disturbance compensation in the design of MPC while ensuring recursive feasibility, robust constraint satisfaction and closed-loop stability.

Motivated by this, we propose a general MPC framework with the disturbance compensation for continuous-time input-affine nonlinear systems with/without the state-dependent disturbance. The disturbance space is divided into two parts: the input-matched one and its orthogonal complement space. The disturbance estimation from the disturbance observer is introduced to alleviate the matched one and the MPC optimization problem is formulated to reject the residual disturbance. Recursive feasibility and regional input-to-state practical stability are guaranteed through strict proofs and the proposed method is applied to a tracking problem for nonholonomic mobile robots. The simulation results verify the effectiveness of the proposed algorithm.

The main contributions are concluded as follows.

1) A nonlinear disturbance observer is employed to capture the state-dependent disturbance. In particular, in the case of traditionally state-independent disturbances, the observer is reduced to an explicit form. The upper bounds of disturbance estimation and estimation error are further derived based on the upper bounds of disturbance and its first derivative, which are suitable for nonvanishing time-varying disturbances.

2) A novel DRMPC framework is developed based on the designed observer. By utilizing the space decomposition method, a disturbance compensation strategy is developed to compensate the matched disturbance actively. The residual disturbance is then restrained through a robust MPC optimization problem with the consideration of the disturbance estimation information including the upper bound of disturbance and its differential. For the case only with matched disturbance, the results can be simplified correspondingly.

3) Theoretical properties include robust constraint satisfaction, recursive feasibility and regional input-to-state practical stability are guaranteed. The proposed DRMPC framework for the regulation problem is naturally extended to the tracking problem for nonholomonic mobile robots. A comparison simulation is provided to show the superiority of the framework.

The remainder of this article is organized as follows. In Section II, the controlled plant, stability objective (i.e., regional ISpS), and disturbance observer are presented, which provides sufficient preliminaries for the design of the DRMPC framework. In Section III, the DRMPC framework is formulated and theoretic analyses, including recursive feasibility and regional ISpS, are provided. In Section IV, the application of the DRMPC framework into nonholonomic mobile robot is proposed as a specified example, the numerical simulation of which is shown in Section V. Finally, Section VI concludes this article and main proofs are in the Appendix for the readers' convenience.

Notations: The sets of reals and nonnegative integers are denoted by $\mathbb{R}$ and $\mathbb{N}$, respectively. For some $r_1 \in \mathbb{R}$, $n_1, n_2 \in \mathbb{N}$ and $n_2 > n_1$, $\mathbb{R}_{>r_1}$, $\mathbb{N}_{\geq n_1}$, $\mathbb{N}_{\leq n_2}$ and $\mathbb{N}_{[n_1,n_2]}$ denote the set $\{r \in \mathbb{R} \mid r > r_1\}$, $\{n \in \mathbb{N} \mid n \geq n_1\}$, $\{n \in \mathbb{N} \mid n \leq n_2\}$ and $\{n \in \mathbb{N} \mid n_1 \leq n \leq n_2\}$, respectively. $\mathbb{R}^n$ denotes the n-dimension vector space. For a matrix M, the set $\lambda(M) = \{\lambda \mid \det(M - \lambda I) = 0\}$ includes its all eigenvalues. Furthermore, its maximum and minimum eigenvalues are denoted by $\bar{\lambda}(M)$ and $\underline{\lambda}(M)$, respectively. A positive definite matrix (semipositive definite matrix) P is denoted by $P > 0$ ($P \geq 0$). For a matrix A of full column rank, the left pseudoinverse of A exists and is defined by $A^\dagger \triangleq (A^\top A)^{-1} A^\top$. For a vector x, $\|x\| \triangleq \sqrt{x^\top x}$ and $\|x\|_P \triangleq \sqrt{x^\top P x}$ with $P \geq 0$ represent the Euclidean norm and P–norm. The bold $\mathbf{0}$ denotes a zero vector of appropriate dimension. A function $\alpha(\cdot) : \mathbb{R}_{\geq 0} \to \mathbb{R}_{\geq 0}$ is called $\mathcal{K}$ function if it is continuous, strictly increasing and $\alpha(0) = 0$. A function $\alpha(\cdot) : \mathbb{R}_{\geq 0} \to \mathbb{R}_{\geq 0}$ is called $\mathcal{K}_\infty$ function if it is a $\mathcal{K}$ function and unbounded ($\alpha(s) \to \infty$ if $s \to \infty$). A function $\beta(\cdot, \cdot) : \mathbb{R}_{\geq 0} \times \mathbb{R}_{\geq 0} \to \mathbb{R}_{\geq 0}$ is called $\mathcal{KL}$ function if, for each fixed $t \geq 0$, $\beta(\cdot, t)$ is a $\mathcal{K}$ function, and, for each fixed $s \geq 0$, $\beta(s, \cdot)$ is decreasing and $\lim_{t\to\infty} \beta(s, t) = 0$. Given a vector $x \in \mathbb{R}^n$ and a compact set Ω, the point-to-set distance is $|x|_\Omega \triangleq \inf\{\|\xi - x\| \mid \xi \in \Omega\}$. Given two sets $\mathcal{A} \subseteq \mathbb{R}^n$, $\mathcal{B} \subseteq \mathbb{R}^n$, the Pontryagin set difference is defined by $\mathcal{A} \sim \mathcal{B} \triangleq \{z \in \mathbb{R}^n \mid z + b \in \mathcal{A},\ \forall b \in \mathcal{B}\}$. Given a signal w, let $\mathbf{w}_{[t_1,t_2]}$ denote a signal defined from time t_1 to time t_2, where the subscript $[t_1, t_2]$ can be omitted when it is inferrable from the context. The set of signals w, the values of which belong to a compact set $\mathcal{W}$, is denoted by $\mathcal{M}_\mathcal{W}$. $\|\mathbf{w}\| \triangleq \sup_{t\geq 0}\{\|w(t)\|\}$ and $\|\dot{\mathbf{w}}\| \triangleq \sup_{t\geq 0}\{\|\dot{w}(t)\|\}$. Define $\mathscr{B}(r) = \{x \in \mathbb{R}^n \mid \|x\|^2 \leq r^2\}$ as a ball of radius r on the Euclidean space. $(\tau|t)$ indicates a variable at time τ predicted from time t.

Moreover, we mark feasible variables satisfying all constraints as $\tilde{\cdot}$ and mark optimal variables obtained by solving an optimal control problem as $\cdot^*$.

II. Problem Formulation

A. Controlled Plant

Consider the following continuous-time nonlinear system with additive bounded disturbances:

$$\dot{x}(t) = \mathscr{F}(x(t), u(t)) + B_w(x)w(t) \tag{1}$$

where the nonlinear component is input-affine with $\mathscr{F}(x(t), u(t)) = f(x) + B(x)u(t)$, and $x(t) \in \mathbb{R}^n$, $u(t) \in \mathbb{R}^m$ and $w(t) \in \mathbb{R}^q$ represent the states, control inputs, and external disturbances, respectively.

Assumption 1: The disturbance and its derivative are assumed to bounded by

$$w(t) \in \mathcal{W} \triangleq \{w(t) \mid \|w(t)\| \leq \eta_1,\ \|\dot{w}(t)\| \leq \eta_2\}$$

where $\eta_1, \eta_2 > 0$ are known constants.

The system is subject to both state and input constraints given by

$$x(t) \in \mathcal{X}, \quad u(t) \in \mathcal{U}, \quad \forall t \geq t_0$$

where $\mathcal{X}$ and $\mathcal{U}$ are compact and convex sets containing the origin in their interior. The disturbance input matrix $B_w(x)$ is bounded by $\|B_w(x)\| \leq \bar{B}_w$ for all $x \in \mathcal{X}$.

Assumption 2: The function $\mathscr{F}(x,u) : \mathbb{R}^n \times \mathbb{R}^m \to \mathbb{R}^n$ with $\mathscr{F}(\mathbf{0},\mathbf{0}) = \mathbf{0}$, is Lipschitz continuous in its first argument $x \in \mathcal{X}$ such that

$$\|\mathscr{F}(x_1,u) - \mathscr{F}(x_2,u)\| \leq \ell \|x_1 - x_2\| \tag{2}$$

for all $x_1, x_2 \in \mathcal{X}$ and $u \in \mathcal{U}$, where ℓ is the Lipschitz constant.

Assumption 3: The matrix $B(x) \in \mathbb{R}^{n\times m}$ is of full column rank regardless of x, i.e., rank$(B(x))$=m.

Remark 1: Assumptions 2 and 3 are compatible with the majority of real input-affine nonlinear systems, such as robot manipulators [24], stirred tank reactors [25], and nonholonomic mobile robots [26].

B. Regional ISpS

In this section, the regional ISpS framework and its Lyapunov-like sufficient conditions are reviewed.

Denote the solution to differential (1) as $\psi(t, x_0, t_0, \mathbf{w})$ with initial state $x(t_0) = x_0$ and initial time $t_0 = 0$.

Definition 1: (Robust positively invariant set): A set $\Psi \subseteq \mathbb{R}^n$ is called a robust positively invariant (RPI) set for system (1) if, for all $x_0 \in \Psi$, it holds that $\psi(t, x_0, t_0, \mathbf{w}) \in \Psi$, for all $\mathbf{w} \in \mathcal{M}_{\mathcal{W}}$.

Definition 2: (Regional ISpS in Ψ): System (1) is said to be input-to-state practical stable in Ψ if Ψ is an RPI set for system (1) and if there exists a $\mathcal{KL}$ function $\tilde{\beta}(\cdot,\cdot)$, a $\mathcal{K}$ function $\tilde{\gamma}(\cdot)$ and a constant $c \geq 0$ such that

$$\|\psi(t, x_0, t_0, \mathbf{w})\| \leq \tilde{\beta}(\|x_0\|, t - t_0) + \tilde{\gamma}(\|\mathbf{w}\|) + c$$

for all $x_0 \in \Psi$ and $t \geq t_0$. Especially, when $c = 0$, system (1) is said to be input-to-state stable in Ψ.

A powerful tool to establish regional ISpS is the comparison function [27], [28]. For system (1), the following ISpS Lyapunov function in Ψ (a type of comparison function) is recalled.

Definition 3: (ISpS Lyapunov function in Ψ): For two given compact sets Θ_w and Ψ with $\{0\} \subset \Theta_w \subseteq \Psi \subseteq \mathbb{R}^n$ and Ψ being an RPI set, a function $V(\cdot,\cdot) : \mathbb{R}_{\geq 0} \times \mathbb{R}^n \to \mathbb{R}_{\geq 0}$ is called an ISpS Lyapunov function in Ψ for system (1) with $w(t) \in \mathcal{W}$, $t \geq t_0$, if it satisfies the following two conditions.

1) (C1) There exist appropriate $\mathcal{K}_\infty$ functions $\alpha_1(\cdot)$, $\alpha_2(\cdot)$ and $\alpha_3(\cdot)$, $\mathcal{K}$ function $\gamma(\cdot)$ and constants $c_1, c_2 \geq 0$ such that, for any $x(t) \in \Psi$ and almost all t

$$V(t, x(t)) \geq \alpha_1(\|x(t)\|) \tag{3}$$

$$V(t, x(t)) \leq \alpha_2(\|x(t)\|) + c_1 \tag{4}$$

$$\begin{aligned}\dot{V}(t, x(t)) &= \frac{\partial V(t, x(t))}{\partial t} + \frac{\partial V(t, x(t))}{\partial x}\frac{\partial x(t)}{\partial t} \\ &\leq -\alpha_3(\|x(t)\|) + \gamma(\|\mathbf{w}\|) + c_2. \end{aligned} \tag{5}$$

For any point t_d of $V(t_d, x(t_d))$, for which (5) does not hold, inequality (5) is replaced by

$$V(t_d^+, x(t_d^+)) \leq V(t_d^-, x(t_d^-)) \tag{6}$$

where t_d^- and t_d^+ are the left and right limits of time instant t_d, respectively.

2) (C2) There exist suitable $\mathcal{K}_\infty$ functions $\alpha_c(\cdot)$ and $\gamma_c(\cdot)$ with $(Id - \gamma_c)(\cdot)$ being a $\mathcal{K}_\infty$ function and a compact set

$$\Theta_w \triangleq \{x(t) \mid V(t, x(t)) \leq \bar{c},\ \forall t \geq t_0\} \tag{7}$$

where $Id(\cdot)$ is the identity function, $\bar{c} \triangleq b(\gamma(\eta_1) + c_3)$, $b(\cdot) \triangleq \alpha_4^{-1} \circ (Id - \gamma_c)^{-1}(\cdot)$, $\alpha_4(\cdot) \triangleq \underline{\alpha}_3 \circ \overline{\alpha}_2^{-1}(\cdot)$, $\underline{\alpha}_3(s) \triangleq \min\{\alpha_3(s/2), \alpha_c(s/2)\}$ and $\overline{\alpha}_2(\cdot) \triangleq \alpha_2(\cdot) + Id(\cdot)$, $c_3 = c_2 + \alpha_c(c_1)$.

Theorem 1 ([29]): For system (1), if it admits an ISpS Lyapunov function associated with sets Θ_w and Ψ, the system is input-to-state practical stable in Ψ and $\lim_{t\to\infty} |\psi(t, x_0, t_0, \mathbf{w})|_{\Theta_w} = 0$.

C. Disturbance Observer

The disturbance $w(t)$ hinders the stabilization for system (1). A natural idea is to design a disturbance observer to estimate the value of disturbance and compensate for disturbance actively. The following disturbance observer is designed to capture the value of $w(t)$:

$$\begin{aligned}\dot{z}(t) &= -L(x)\left[B_w(x)(\phi(x) + z(t)) + f(x) + B(x)u(t)\right] \\ \hat{w}(t) &= z(t) + \phi(x)\end{aligned} \tag{8}$$

where $\hat{w}(t) \in \mathbb{R}^q$ is the disturbance estimation, $z(t) \in \mathbb{R}^q$ is an auxiliary variable, $\phi(x) \in \mathbb{R}^q$ is a nonlinear function to be designed, and $L(x) = \frac{\partial \phi(x)}{\partial x^\top} \in \mathbb{R}^{q\times n}$ is the observer gain. The initial value of $\hat{w}(t)$ is set as $\hat{w}(0) = \mathbf{0}$.

Define disturbance estimation error $w_s(t) \triangleq w(t) - \hat{w}(t)$. Combined with system (1), the disturbance estimation error dynamics can be described as

$$\dot{w}_s(t) = \dot{w}(t) - L(x)B_w(x)w_s(t). \tag{9}$$

Lemma 1 ([13]): The disturbance estimation error dynamics (9) is locally input-to-state stable if the observer gain $L(x)$ is appropriately chosen such that the system

$$\dot{w}_s(t) = -L(x)B_w(x)w_s(t) \tag{10}$$

is asymptotically stable.

Under the condition in Lemma 1, it is clear that the definition of input-to-state stability ensures the boundedness of $\|w_s\|$. In particular, for some specific systems, the bound on it can be derived explicitly, which is detailed in Lemma 2.

Lemma 2: For some specific $B_w(x)$, if there exists $L(x)$ such that $-L(x)B_w(x)$ is independent of x, that is $-L(x)B_w(x)$ is a constant matrix denoting as ψ, and ψ is Hurwitz, then

$$\|w_s(t)\| \leq \beta(\psi)\left(\eta_1 - \frac{\eta_2}{c(\psi)}\right)e^{-c(\psi)t} + \frac{\eta_2\beta(\psi)}{c(\psi)}$$

$$\|\hat{w}(t)\| \leq \frac{\eta_1\|\psi\|\beta(\psi)}{c(\psi)}(1 - e^{-c(\psi)t})$$

where $\beta(\psi) \triangleq \sqrt{\|Y^{-1}\|\|Y\|}$, $c(\psi) \triangleq 1/(2\|Y\|)$ and Y is the unique Hermitian matrix obtained by solving the Lyapunov equation $Y\psi + \psi^\top Y = -I$.

Proof: By considering the initial condition $w_s(0) = w(0)$, the solution for (9) is

$$w_s(t) = e^{\psi t} w(0) + \int_0^t e^{\psi(t-s)} \dot{w}(s) ds.$$

Therefore

$$\begin{aligned} \|w_s(t)\| &\le \left\|e^{\psi t}\right\| \|w(0)\| + \int_0^t \left\|e^{\psi(t-s)}\right\| \|\dot{w}(s)\| \, ds \\ &\le \eta_1 \beta(\psi) e^{-c(\psi)t} + \eta_2 \int_0^t \beta(\psi) e^{-c(\psi)(t-s)} ds \\ &= \beta(\psi) \left(\eta_1 - \frac{\eta_2}{c(\psi)}\right) e^{-c(\psi)t} + \frac{\eta_2 \beta(\psi)}{c(\psi)} \end{aligned}$$

where the second inequality follows from Lemma 8 in Appendix A.

Furthermore, disturbance observer (8) implies that

$$\dot{\hat{w}}(t) = \psi \hat{w}(t) - \psi w(t). \tag{11}$$

Because of $\hat{w}(0) = \mathbf{0}$, the solution for (11) is

$$\hat{w}(t) = \int_0^t -e^{\psi(t-s)} \psi w(s) ds$$

and therefore, from Lemma 8 in Appendix A

$$\begin{aligned} \|\hat{w}(t)\| &\le \eta_1 \|\psi\| \int_0^t \left\|e^{\psi(t-s)}\right\| ds \\ &\le \eta_1 \|\psi\| \int_0^t \beta(\psi) e^{-c(\psi)(t-s)} ds \\ &= \frac{\eta_1 \|\psi\| \beta(\psi)}{c(\psi)} (1 - e^{-c(\psi)t}). \end{aligned}$$

Remark 2: The matrix $L(x)$ satisfying the condition in Lemma 2 can be found for some classes of systems. Take the nonholonomic mobile robot subject to sideslip disturbances as an example. For the disturbance matrix $B_w(x) = \begin{bmatrix} \cos x_3 & -\sin x_3 \\ \sin x_3 & \cos x_3 \\ 0 & 0 \end{bmatrix}$, the corresponding observer gain can be chosen as $L(x) = L_1 \begin{bmatrix} \cos x_3 \sin x_3 - x_1 \sin x_3 + x_2 \cos x_3 \\ -\sin x_3 \cos x_3 - x_1 \cos x_3 - x_2 \sin x_3 \end{bmatrix}$, which will be discussed in Section IV as an application of the proposed method. Moreover, for disturbance matched systems with $B_w(x) = B(x)$, it is generally the case that the input matrices are constant, which implies the satisfaction of Lemma 2.

Remark 3: The proof of Lemma 2 states that the upper bound on $\|w_s(t)\|$ and $\|\hat{w}(t)\|$ can be estimated by virtue of the upper bound on the norm of matrix exponential. More than five estimation methods for the matrix exponential are provided in [30] and their estimation precisions highly depend on the property of matrix ψ. In this article, the norm bound in Lemma 8 is used and can be replaced in other specific cases.

Remark 4: Various disturbances in engineering can be described by an exogenous system [31]

$$\begin{aligned} \dot{\sigma}(t) &= W\sigma(t) + Mw_1(t) \\ w(t) &= V\sigma(t) \end{aligned}$$

where $w_1(t)$ is bounded in $\mathscr{H}_2$-norm and matrices W, V, M are of compatible dimensions. By the disturbance observer of $\sigma(t)$

$$\begin{aligned} \dot{z}(t) &= (W - L(x)B_w(x)V)(z(t) + \phi(x)) \\ &\quad - L(x)(f(x) + B(x)u(t)) \\ \hat{\sigma}(t) &= z(t) + \phi(x) \end{aligned}$$

the estimation error system can be described as

$$\dot{\sigma}_s(t) = (W - L(x)B_w(x)V)\sigma_s(t) + Mw_1(t) \tag{12}$$

where $\sigma_s(t) \triangleq \sigma(t) - \hat{\sigma}(t)$. Therefore, the estimation error dynamics (12) can be handled analogously to dynamics (9). Defining $\hat{w}(t) = V\hat{\sigma}(t)$ and then $w_s(t) = V\sigma_s(t)$, the upper bound on $w_s(t)$ can therefore be given by the upper bound on $\sigma_s(t)$.

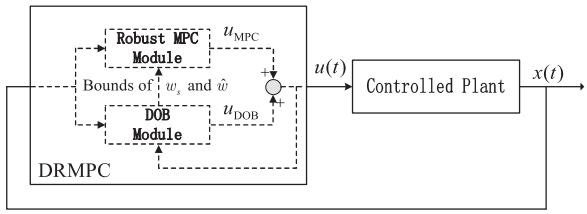

Fig. 1. Block diagram of the DRMPC framework.

III. Disturbance Rejection MPC Framework

The main control objective of this article is to steer the state to a neighborhood of the origin. To achieve this goal, a DRMPC framework is proposed and the controller is composed of two parts: the optimal control input $u_{\text{MPC}}(t)$ and the disturbance compensation input $u_{\text{DOB}}(t)$, i.e.,

$$u(t) = u_{\text{MPC}}(t) + u_{\text{DOB}}(t). \tag{13}$$

Therein, the former part $u_{\text{MPC}}(t)$ is obtained by solving the optimal control problem to achieve desirable control performance and the latter one $u_{\text{DOB}}(t)$ is designed to alleviate the effect of disturbances based on the DOB.

The block diagram of the DRMPC framework is shown in Fig. 1.

A. Design of Disturbance Compensation Input u_{DOB}

Define $\mathscr{G} \triangleq \{s \mid B^\top(x)s = 0\}$ and $\mathscr{G}^\perp \triangleq \{\zeta \mid \forall s \in \mathscr{G},\ s^\top \zeta = 0\}$ as the nullspace of $B^\top(x)$ and the orthogonal complement of space $\mathscr{G}$, respectively. Take matrices U_1 and U_2 such that

$$\begin{aligned} \mathscr{G}^\perp &= \text{span}\{U_{1,i}(x) \mid i = 1, 2, \ldots, m\} \\ \mathscr{G} &= \text{span}\{U_{2,j}(x) \mid j = 1, 2, \ldots, n-m\} \end{aligned}$$

where the matrix subscripts i, j stand for the ith and jth column of matrix $U_1(x)$ and $U_2(x)$, respectively. Without loss of generality, let $U_{1,i}$ and $U_{2,j}$ be orthonormal vectors and admit $U_{2,j} = \mathbf{0}$ only when $n = m$. It follows from the fact $I_n = B(x)B^\dagger(x) + U_2(x)U_2^\dagger(x)$ that $B_w(x)w(t) = B(x)B^\dagger(x)B_w(x)w(t) + U_2(x)U_2^\dagger(x)B_w(x)w(t)$. Define $h(t) \triangleq B^\dagger(x)B_w(x)w(t)$ and $g(t) \triangleq U_2(x)U_2^\dagger(x)B_w(x)w(t)$, then system (1) can be rewritten as

$$\dot{x}(t) = f(x) + B(x)\left(u(t) + h(t)\right) + g(t). \tag{14}$$

Define $T(x) \triangleq [U_2(x), U_1(x)]^\top$, which is orthogonal and satisfies $T^{-1}(x) = T^\top(x) = [U_2(x), U_1(x)]$. Premultiply (14)

by $T(x)$ and we obtain

$$T(x)\dot{x} = T(x)f(x) + \begin{bmatrix} 0 \\ U_1^\top(x)B(x) \end{bmatrix}(u(t)+h(t)) + \begin{bmatrix} U_2^\top(x) \\ 0 \end{bmatrix} g(t). \tag{15}$$

This implies that only $h(t)$ can be compensated for by control input $u(t)$. Therefore, the disturbance compensation input $u_{\text{DOB}}(t)$ is designed as

$$u_{\text{DOB}}(t) \triangleq -\hat{h}(t) \tag{16}$$

with $\hat{h}(t) \triangleq B^\dagger(x)B_w(x)\hat{w}(t)$. In this setting, substitute $u(t)$ in (13) into system (14) and the resulting closed-loop system is given by

$$\dot{x}(t) = f(x) + B(x)u_{\text{MPC}}(t) + B_w(x)w_s(t) + \hat{g}(t) \tag{17}$$

with $\hat{g}(t) \triangleq U_2(x)U_2^\dagger(x)B_w(x)\hat{w}(t) = U_2(x)U_2^\top(x)B_w(x)\hat{w}(t)$.

B. Design of Optimal Control Input u_{MPC}

The optimal control input $u_{\text{MPC}}(t)$ is implemented to reject the disturbance component $B_w(x)w_s(t) + \hat{g}(t)$ in (17) and guarantee a desirable control performance, which is computed by solving an optimal control problem at each sampling instant t_k, $k \in \mathbb{N}$. Denote the sampling interval as δ, then sampling instants satisfy $t_{k+1} - t_k = \delta$. The optimal control problem at t_k with prediction horizon T is formulated as follows.

Problem 1:

$$\min_{\bar{u}(\cdot)} J(x(t_k), \bar{u}(\cdot), T) \tag{18}$$

subject to

$$\bar{x}(t_k|t_k) = x(t_k) \tag{18a}$$

$$\dot{\bar{x}}(\tau|t_k) = f(\bar{x}) + B(\bar{x})\bar{u}(\tau|t_k) \tag{18b}$$

$$\bar{u}(\tau|t_k) \in \bar{\mathcal{U}} \tag{18c}$$

$$\bar{x}(\tau|t_k) \in \bar{\mathcal{X}}(\tau - t_k) \tag{18d}$$

$$\bar{x}(t_k + T|t_k) \in \mathcal{X}_f \tag{18e}$$

with $\tau \in [t_k, t_k + T]$. $\bar{\mathcal{U}} \triangleq \mathcal{U} \sim \mathscr{B}(\varrho)$, $\varrho \triangleq \max_{x\in\mathcal{X}} \|B^\dagger(x)B_w(x)\| \frac{\eta_1 \|\psi\| \beta(\psi)}{c(\psi)}$ and $\bar{\mathcal{X}}(\tau - t_k) \triangleq \mathcal{X} \sim \mathcal{B}(\tau - t_k)$ are the tightened constraint sets to guarantee closed-loop constraint satisfaction (analogously in [32]). $\mathcal{B}(s) \triangleq \{x \in \mathbb{R}^n \mid \|x\| \le \frac{\varpi_m}{\ell}(e^{\ell s} - 1)\}$, $\varpi_m \triangleq \varpi(t_0, \infty)$ will be defined in Lemma 3 and $\mathcal{X}_f \triangleq \{s \mid \|s\|_P^2 \le \varepsilon^2\}$ is the terminal constraint set.

The cost function $J(x(t_k), \bar{u}(\cdot), T)$ in Problem 1 is defined by

$$J(x(t_k), \bar{u}(\cdot), T) \triangleq \int_{t_k}^{t_k+T} F(\bar{x}(\tau|t_k), \bar{u}(\tau|t_k))d\tau + V_f(\bar{x}(t_k + T|t_k))$$

in which $F(\cdot,\cdot) : \mathbb{R}^n \times \mathbb{R}^m \to \mathbb{R}_{\ge 0}$ is the stage cost function to evaluate the control performance and energy loss for the control process and $V_f(\cdot) : \mathbb{R}^n \to \mathbb{R}_{\ge 0}$ is the terminal cost function to penalize the undesired terminal state. The stage and terminal cost functions are defined in the quadratic form, that is, $F(\bar{x}, \bar{u}) = \|\bar{x}\|_Q^2 + \|\bar{u}\|_R^2$ and $V_f(\bar{x}) = \|\bar{x}\|_P^2$ with weighting matrices $Q \ge 0$, $R > 0$ and $P \ge 0$.

By solving Problem 1, the optimized input trajectory $\bar{u}^*(\tau|t_k)$ and optimized state trajectory $\bar{x}^*(\tau|t_k)$ are obtained for all $\tau \in [t_k, t_k + T]$. The optimal control input $u_{\text{MPC}}(t)$ is then set as

$$u_{\text{MPC}}(t) = \bar{u}^*(t|t_k)$$

for $t \in [t_k, t_{k+1})$.

Assumption 4: For nominal system $\dot{\bar{x}}(t) = f(\bar{x}) + B(\bar{x})\bar{u}(t)$, there exists a set $\mathcal{X}_r \triangleq \{\bar{x} \mid V_f(\bar{x}) \le r^2\} \subseteq \mathcal{X}$ with $r > 0$ and a local stabilizing controller $\kappa_f(\bar{x}) = K\bar{x}$ such that by implementing the controller $\kappa_f(\bar{x})$ for all $\bar{x} \in \mathcal{X}_r$, it holds that $\kappa_f(\bar{x}) \in \bar{\mathcal{U}}$ and

$$\dot{V}_f(\bar{x}) + F(\bar{x}, \kappa_f(\bar{x})) \le 0. \tag{19}$$

Remark 5: There are several approaches to obtain the local stabilizing region $\mathcal{X}_r$ and controller $\kappa_f(\bar{x})$ satisfying Assumption 4, such as linearization methods in [33] and [34] and feedback linearization methods in [35].

The implementation of the DRMPC framework.

i) Set $k = 0$. Initialize the systems and sample the initial state $x(t_k)$.
ii) Solve Problem 1 and obtain the optimal control input $u_{\text{MPC}}(t)$ for $t \in [t_k, t_{k+1})$.
iii) For $t \in [t_k, t_{k+1})$, apply $u(t) = u_{\text{MPC}}(t) + u_{\text{DOB}}(t)$ to the real system (1), where $u_{\text{DOB}}(t) = -B^\dagger(x)B_w(x)\hat{w}(t)$ is obtained continuously by dynamics (8).
iv) When $t = t_{k+1}$, set $k = k + 1$ and go back to (ii).

C. Theoretical Analysis

The following two lemmas are useful for the proof of recursive feasibility in Theorem 2.

Lemma 3: For any sampling instant t_k, suppose that the closed-loop system (17) is controlled by control law (13) and the predicted system (18b) is controlled by the optimal solution $\bar{u}^*(\tau|t_k)$ from the same initial state, i.e. $x(t_k) = \bar{x}^*(t_k|t_k)$. Then the deviation between the actual state trajectory $x(\tau)$ and predicted optimal state trajectory $\bar{x}^*(\tau|t_k)$ is norm bounded, for $\tau \in [t_k, t_k + T]$, by

$$\|x(\tau) - \bar{x}^*(\tau|t_k)\| \le \frac{\varpi(t_k, \tau)}{\ell}\left(e^{\ell(\tau - t_k)} - 1\right) \tag{20}$$

where $\varpi(t_k, \tau) \triangleq \sup_{s\in[t_k,\tau]} \bar{B}_w(\|w_s(s)\| + \|\hat{w}(s)\|)$ and ℓ is the Lipschitz constant of function $\mathscr{F}(x, u)$ with respect to x.

Proof: The difference between the actual state and predicted optimal state resulting from disturbance $w(t)$ can be expressed as

$$\begin{aligned} &\|x(\tau) - \bar{x}^*(\tau|t_k)\| \\ &= \|x(t_k) + \int_{t_k}^{\tau} \mathscr{F}(x(s), u(s)) + B_w(x)w(s)ds \\ &\quad - \bar{x}^*(t_k|t_k) - \int_{t_k}^{\tau} \mathscr{F}(\bar{x}^*(s|t_k), \bar{u}^*(s|t_k))ds\| \\ &\overset{(1)}{\le} \int_{t_k}^{\tau} \|\mathscr{F}(x(s), \bar{u}^*(s|t_k)) - \mathscr{F}(\bar{x}^*(s|t_k), \bar{u}^*(s|t_k))\|ds \end{aligned}$$

$$
\begin{aligned}
&+\int_{t_k}^{\tau}\|B_w(x)w(s)-B(x)\hat{h}(s)\|ds\\
&\overset{(16)}{=}\int_{t_k}^{\tau}\|\mathscr{F}(x(s),\bar{u}^*(s|t_k))-\mathscr{F}(\bar{x}^*(s|t_k),\bar{u}^*(s|t_k))\|ds\\
&\quad+\int_{t_k}^{\tau}\|B_w(x)w_s(s)+U_2(x)U_2^{\dagger}(x)B_w(x)\hat{w}(s)\|ds\\
&\le\varpi(t_k,\tau)(\tau-t_k)+\ell\int_{t_k}^{\tau}\|x(s)-\bar{x}^*(s|t_k)\|ds\\
&\le\frac{\varpi(t_k,\tau)}{\ell}\left(e^{l(\tau-t_k)}-1\right)
\end{aligned}
$$

where the last two inequalities follows from (38) in Lemma 9 and (41) in Lemma 10 of Appendix A.

Lemma 4: For $\tau\in[t_{k+1},t_k+T)$ and any $x,y\in\mathbb{R}^n$, if $x\in\mathcal{X}\sim\mathcal{B}(\tau-t_k)$ satisfying $\|y-x\|\le\frac{\varpi_m}{\ell}(e^{\ell\delta}-1)e^{\ell(\tau-t_{k+1})}$, then it holds that $y\in\mathcal{X}\sim\mathcal{B}(\tau-t_{k+1})$.

Proof: For any $s\in\mathcal{B}(\tau-t_{k+1})$, it holds that $\|s\|\le\frac{\varpi_m}{\ell}(e^{\ell(\tau-t_{k+1})}-1)$. Define auxiliary variables $z=y-x+s$. It follows from the triangle inequality that $\|z\|\le\|y-x\|+\|s\|\le\frac{\varpi_m}{\ell}(e^{\ell\delta}-1)e^{\ell(\tau-t_{k+1})}+\frac{\varpi_m}{\ell}(e^{\ell(\tau-t_{k+1})}-1)\le\frac{\varpi_m}{\ell}(e^{\ell(\tau-t_k)}-1)$, which implies $z\in\mathcal{B}(\tau-t_k)$. Since $x\in\mathcal{X}\sim\mathcal{B}(\tau-t_k)$ and $z\in\mathcal{B}(\tau-t_k)$, it follows from the definition of the Pontryagin set difference $\mathcal{X}\sim\mathcal{B}(\tau-t_k)$ that $x+z\in\mathcal{X}$, which implies $y+s=x+z\in\mathcal{X}$. Further, from the fact that $y+s\in\mathcal{X}$ holds for any $s\in\mathcal{B}(\tau-t_{k+1})$, we have $y\in\mathcal{X}\sim\mathcal{B}(\tau-t_{k+1})$ directly by the definition of the Pontryagin set difference.

Theorem 2: For system (1), Problem 1 under the proposed DRMPC framework is recursively feasible for all sampling time t_k, $k\in\mathbb{N}$, if Problem 1 is feasible at the initial time t_0 and the following conditions are satisfied:

$$\text{(i)}\ \overline{\lambda}(\sqrt{P})\frac{\varpi_m}{\ell}\left(e^{\ell\delta}-1\right)e^{\ell(T-\delta)}\le r-\varepsilon; \tag{21}$$

$$\text{(ii)}\ \frac{\underline{\lambda}(Q^*)\delta}{2\overline{\lambda}(P)}\ge\ln\frac{r}{\varepsilon}; \tag{22}$$

$$\text{(iii)}\ \mathcal{X}_r\subseteq\mathcal{X}\sim\mathcal{B}(T) \tag{23}$$

with $Q^*=Q+K^\top RK$.

Theorem 3: Under the proposed DRMPC framework, the resulting closed-loop system (17) is regional input-to-state practical stable, which implies the regional ISpS for system (1).

For the sake of readability, the proofs of Theorems 2 and 3 are located in Appendix B.

Remark 6: The DRMPC framework in this article can be modified and applied to discrete-time systems straightforward. Since the $\mathcal{K}_\infty$ function $\alpha_2(\|x\|)=\nu\underline{\lambda}(P)\|x\|^2$, $\nu>1$ (with $c_1=0$) in (4) can be obtained by referring to [1, Lemma 2.15 and Prop. 2.18], and $(\|\mathbf{w}\|+\|\delta\mathbf{w}\|)$ can be considered as total disturbances (with $c_2=0$), the closed-loop system is input-to-state stable regarding $(\|\mathbf{w}\|+\|\delta\mathbf{w}\|)$, where $\|\delta\mathbf{w}\|$ is the admissible maximal difference between two discrete time instants corresponding to $\|\dot{\mathbf{w}}\|$ in this article.

D. State-Independent Addictive Disturbance

If the disturbance input matrix $B_w(x)$ in (1) is fixed as a constant matrix B_w, that is

$$\dot{x}(t)=f(x)+B(x)u(t)+B_ww(t) \tag{24}$$

then the theoretical results derived above still hold by making some slight modifications. Specifically, the result in Lemma 2 can be reduced to the following corollary.

Corollary 1: Suppose the disturbance input matrix B_w is of full column rank. For system (24) and error dynamics (9), choose $L(x)=k_LB_w^{\dagger}$ and $\phi(x)=k_LB_w^{\dagger}x$ such that $\psi=-k_LI_n$ with $k_L>0$. Then, the upper bounds on disturbance estimation error $w_s(t)$ and disturbance estimation $\hat{w}(t)$ are given by $\|w_s(t)\|\le(\eta_1-\frac{\eta_2}{k_L})e^{-k_Lt}+\frac{\eta_2}{k_L}$ and $\|\hat{w}(t)\|\le\eta_1(1-e^{-k_Lt})$.

When the disturbance is matched and $\eta_1\ge\frac{\eta_2}{k_L}$, take $\varpi_m(t_k)=\bar{B}_w((\eta_1-\frac{\eta_2}{k_L})e^{-k_Lt_k}+\frac{\eta_2}{k_L})$ instead of ϖ_m in the constraint (18d) and condition (21). Then, the constraint (18d) can be relaxed step by step as time goes by. The theoretical properties obtained in Section III-C (i.e., Lemma 3, Lemma 4, Theorem 2, and Theorem 3) still hold with less conservativeness.

Remark 7: If the conditions in Lemma 2 and Corollary 1 are not satisfied, the disturbance observer can also be designed as

$$
\begin{aligned}
\dot{v}(t)&=-k_L\left[v(t)+k_Lx(t)+f(x)+B(x)u(t)\right]\\
\hat{\varsigma}&=v(t)+k_Lx(t)
\end{aligned}
$$

by considering $\varsigma\triangleq B_w(x)w(t)$. All these observers are compatible with the DRMPC framework without no essential difference.

For specific cases, such as the Lipschitz nonlinear systems [36] and linear systems [37], the tube MPC method can be utilized to design $u_{\text{MPC}}(t)$ in (17) by making a small modification, which implies that the proposed DRMPC framework is of universal significance and is applicable to a general class of systems.

IV. Application to Nonholonomic Mobile Robots

In this section, we demonstrate the applicability of the proposed DRMPC framework by a specific application, which provides an insight to interact the DRMPC framework with existing advanced studies. Specifically, we focus on the trajectory tracking problem of a nonholonomic mobile robot, which is of great interest in robots and MPC realms [26], [38]. The proposed DRMPC framework generalizes and improves the algorithm for nonholonomic mobile robots with matched disturbances in [23].

A. Physical Model

The nonholonomic mobile robot shown in Fig. 2(a) can be formulated by the following dynamics:

$$\dot{x}(t)=\mathscr{F}(x(t),u(t))=\begin{bmatrix}\cos\theta&0\\\sin\theta&0\\0&1\end{bmatrix}\begin{bmatrix}v\\\omega\end{bmatrix} \tag{25}$$

where $x=[p^\top,\theta]^\top\in\mathbb{R}^2\times(-\pi,\pi]$ is the system state with position vector $p=[x_1,x_2]^\top$ and orientation angle θ, and $u=[v,\omega]^\top$ is the control input with linear velocity v and angular velocity ω.

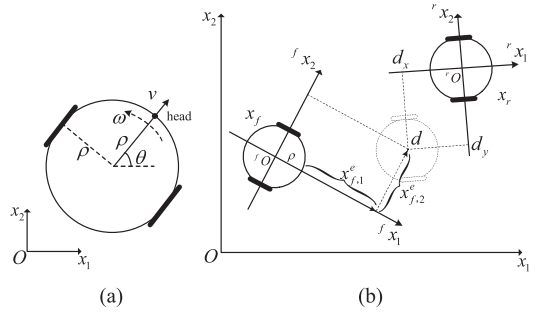

Fig. 2. Nonholonomic system and the formation configuration. (a) Unicycle-type mobile robot. (b) Leader–follower configuration.

Denote v^L and v^R as the velocities of driving wheels on the left and right sides, respectively. The linear velocity v and angular velocity ω can then be described by $v = (v^L + v^R)/2$ and $\omega = (v^R - v^L)/2\rho$, where ρ is the radius of robot. Because the velocities of driving wheels are bounded by $|v^L| \le a$ and $|v^R| \le a$, the control input u should satisfy the diamond-shaped constraint $\mathcal{U} = \{[v, \omega]^\top \mid \frac{|v|}{a} + \frac{|\omega|}{b} \le 1\}$ with $b = a/\rho$.

B. Leader–Follower Formation

Different from the regulation problem to a fixed point, it is necessary to introduce the reference trajectory for tracking problem. In particular, we consider the leader–follower formation as shown in Fig. 2(b). Therein, the state trajectory x_r of the leader is generated by the following nominal system:

$$\dot{x}_r(t) = \mathscr{F}(x_r(t), u_r(t))$$

where all variables represent the same meanings in the physical model (25) with subscript r. The state trajectory x_f of the follower is perturbed and its head position is required to follow a virtual point $d = [d_x, d_y]^\top$ regarding the Frenet–Serret frame ${}^rO$ fixed on the leader.

Fig. 2(a) displays the head position of the mobile robot. The dynamics of the head position for the follower can be described by

$$\begin{aligned}\dot{x}_f(t) &= \mathscr{F}_h(x_f(t), u_f(t)) + B_w(x_f)w(t)\\ &= B(x_f)u_f(t) + B_w(x_f)w(t)\end{aligned} \tag{26}$$

where $x_f = [p_f^\top, \theta_f]^\top \in \mathbb{R}^2 \times (-\pi, \pi]$ is the state with $p_f = [x_{f,1}, x_{f,2}]^\top$, $u_f = [v_f, w_f]^\top$ is the control input satisfying input constraint $u_f \in \mathcal{U}$, the input matrix $B(x_f)$ is state-dependent

$$B(x_f) = \begin{bmatrix}\cos\theta_f & -\rho\sin\theta_f\\ \sin\theta_f & \rho\cos\theta_f\\ 0 & 1\end{bmatrix} \tag{27}$$

$B_w(x_f) \in \mathbb{R}^{3\times q}$ is the disturbance input matrix and $w(t) \in \mathbb{R}^q$ is the external bounded disturbance satisfying $\|w(t)\| \le \eta_1$ and $\|\dot{w}(t)\| \le \eta_2$. In real-life problems, the disturbance is mainly induced by the sideslip, hence the perturbations on the angular velocity are neglected and let $B_w(x_f)w(t) = [\xi_1(t), \xi_2(t), 0]^\top \in \mathbb{R}^3$ with the third component being 0. The nominal form of system (26) can be expressed as

$$\dot{\bar{x}}_f(t) = \mathscr{F}_h(\bar{x}_f(t), \bar{u}_f(t)). \tag{28}$$

Define the rotation matrix as

$$R(\theta_f) = \begin{bmatrix}\cos\theta_f & -\sin\theta_f\\ \sin\theta_f & \cos\theta_f\end{bmatrix}.$$

The tracking error p_f^e from follower position p_f to virtual point d [see Fig. 2(b)] can be given by

$$p_f^e = \begin{bmatrix}x_{f,1}^e\\ x_{f,2}^e\end{bmatrix} = R(-\theta_f)\begin{bmatrix}x_{r,1} - x_{f,1}\\ x_{r,2} - x_{f,2}\end{bmatrix} + R(\theta_{rf})\begin{bmatrix}d_x\\ d_y\end{bmatrix}$$

where $x_{r,1}$ and $x_{r,2}$ are the first two components of x_r, and $\theta_{rf} \triangleq \theta_r - \theta_f$. Taking the derivative of p_f^e, the tracking error dynamics can be generated by

$$\dot{p}_f^e = \begin{bmatrix}\dot{x}_{f,1}^e\\ \dot{x}_{f,2}^e\end{bmatrix} = \Phi p_f^e + u_f^e + H(\theta_f)B_w(x_f)w(t) \tag{29}$$

in which

$$\Phi = \begin{bmatrix}0 & \omega_f\\ -\omega_f & 0\end{bmatrix},\ H(\theta_f) = \begin{bmatrix}-\cos\theta_f & -\sin\theta_f & 0\\ \sin\theta_f & \cos\theta_f & 0\end{bmatrix}$$

$$u_f^e = \begin{bmatrix}v_f^e\\ \omega_f^e\end{bmatrix} = \begin{bmatrix}-v_f + (v_r - d_y\omega_r)\cos\theta_{rf} - d_x\omega_r\sin\theta_{rf}\\ -\rho\omega_f + (v_r - d_y\omega_r)\sin\theta_{rf} + d_x\omega_r\cos\theta_{rf}\end{bmatrix}.$$

The corresponding nominal form of (29) is

$$\dot{\bar{p}}_f^e = \begin{bmatrix}\dot{\bar{x}}_{f,1}^e\\ \dot{\bar{x}}_{f,2}^e\end{bmatrix} = \Phi\bar{p}_f^e + \bar{u}_f^e. \tag{30}$$

In the leader–follower configuration, the tracking task can be achieved by driving the tracking error p_f^e to a neighborhood of the origin. In the following, we review some preliminaries for the leader–follower problem formulated above.

Lemma 5: The function $\mathscr{F}_h(\bar{x}_f, \bar{u}_f) : \mathbb{R}^2 \times (-\pi, \pi] \times \mathcal{U} \to \mathbb{R}^2 \times (-\pi, \pi]$ in nominal system (28) is locally Lipschitz continuous with respect to $\bar{x}_f$ with a Lipshitz constant $\ell = a$.

Proof: For the same input u and different states x_q and x_p

$$\begin{aligned}&\|\mathscr{F}_h(x_q, u) - \mathscr{F}_h(x_p, u)\|^2\\ &= v^2(\cos\theta_q - \cos\theta_p)^2 + \rho^2\omega^2(\sin\theta_q - \sin\theta_p)^2\\ &\quad + v^2(\sin\theta_q - \sin\theta_p)^2 + \rho^2\omega^2(\cos\theta_q - \cos\theta_p)^2\\ &= 2(v^2 + \rho^2\omega^2)(1 - \cos(\theta_q - \theta_p))\\ &\le 4\max\{v^2 + \rho^2\omega^2\}\sin^2\frac{(\theta_q - \theta_p)}{2}\\ &\le \max\{v^2 + \rho^2\omega^2\}(\theta_q - \theta_p)^2\\ &\le a^2\|x_q - x_p\|^2\end{aligned} \tag{31}$$

where the maximum of $(v^2 + \rho^2\omega^2)$, subject to constraint $\frac{|v|}{a} + \frac{|\omega|}{b} \le 1$, is reached at the vertexes of constraint set $\mathcal{U}$. The inequality (31) implies $\|\mathscr{F}_h(x_q, u) - \mathscr{F}_h(x_p, u)\| \le \ell\|x_q - x_p\|$ with the Lipshitz constant $\ell = a$.

Remark 8: It is clear that the function $\mathscr{F}_h(x_f, u_f)$ in (26) and the matrix $B(x_f)$ in (27) satisfy Assumption 2 and Assumption 3, hence it permits the implementation of the proposed DRMPC framework to the formulated tracking problem.

The following lemma gives additional constraints on the input of the leader in order to realize the leader–follower formation.

Lemma 6 (see [35]): For the leader robot with the control input $u_r = [v_r, \omega_r]^\top \in \mathcal{U}$, there exists control input $u_f = [v_f, \omega_f]^\top \in \mathcal{U}$ for the follower robot such that the state of

the follower is able to track the specific position $d = (d_x, d_y)$ with respect to the leader, if the control input of the leader is bounded by $\|u_r\| \leq \frac{a}{\sqrt{2}\|M\|}$ with $\|M\| = \left[\begin{smallmatrix} 1 & -d_y \\ 0 & d_x \end{smallmatrix}\right]$. Furthermore, the corresponding control input for the follower can be given by $u_f^d = [v_f^d, \omega_f^d]^\top = \Lambda R(\theta_{rf}) M u_r$ with $\Lambda = \text{diag}\{1, \frac{1}{\rho}\}$, and there exists a positive constant γ such that $\frac{|v_f^d|}{a} + \frac{|\omega_f^d|}{b} \leq \gamma$ with $\gamma \in [\max\{\|u_r\|\}\frac{\sqrt{2}\|M\|}{a}, 1)$.

C. Controller Design

First, design the disturbance compensation input $u_{\text{DOB}}(t)$ based on the method presented in Section III-A. By letting matrices

$$U_1(x_f) = \begin{bmatrix} \frac{-\rho\sin\theta_f}{\sqrt{\rho^2+1}} & \cos\theta_f \\ \frac{\rho\cos\theta_f}{\sqrt{\rho^2+1}} & \sin\theta_f \\ \frac{1}{\sqrt{\rho^2+1}} & 0 \end{bmatrix},\ U_2(x_f) = \begin{bmatrix} \frac{\sin\theta_f}{\sqrt{\rho^2+1}} \\ \frac{-\cos\theta_f}{\sqrt{\rho^2+1}} \\ \frac{\rho}{\sqrt{\rho^2+1}} \end{bmatrix}$$

system (26) can be decomposed analogous to (15). The disturbance compensation input is therefore given as

$$u_{\text{DOB}}(t) = -B^\dagger(x_f) B_w(x_f) \hat{w}(t)$$

where $\hat{w}(t)$ is the disturbance estimation from disturbance observer (8) with slight modifications. The resulting closed-loop tracking error system (29) can be rewritten as

$$\dot{p}_f^e = \Phi p_f^e + u_{\text{MPC}}^e + H(\theta_f)\left(B_w(x_f) w_s(t) + \hat{g}(t)\right) \tag{32}$$

where

$$u_{\text{MPC}}^e = \begin{bmatrix} -v_{\text{MPC}} + (v_r - d_y\omega_r)\cos\theta_{rf} - d_x\omega_r\sin\theta_{rf} \\ -\rho\omega_{\text{MPC}} + (v_r - d_y\omega_r)\sin\theta_{rf} + d_x\omega_r\cos\theta_{rf} \end{bmatrix}$$

and $\hat{g}(t) = U_2(x_f)U_2^\top(x_f)B_w(x_f)\hat{w}(t)$.

The remaining step is to find the optimal control input $u_{\text{MPC}}(t) = [v_{\text{MPC}}(t), \omega_{\text{MPC}}(t)]^\top$ such that error system (32) is stable with a desired control performance. The optimal control input $u_{\text{MPC}}(t)$ for $t \in [t_k, t_{k+1})$ is chosen as the first portion of optimal solution $\bar{u}_f^*(t|t_k)$ to the following optimization problem.

Problem 2:

$$\min_{\bar{u}_f(\cdot)} \quad J(\bar{p}_f^e(t_k), \bar{u}_f(\cdot), T) \tag{33}$$

subject to

$$\bar{x}_f(t_k|t_k) = x_f(t_k) \tag{33a}$$

$$\dot{\bar{x}}_f(\tau|t_k) = \mathscr{F}_h(\bar{x}_f(\tau|t_k), \bar{u}_f(\tau|t_k)) \tag{33b}$$

$$\bar{u}_f(\tau|t_k) \in \bar{\mathcal{U}} \tag{33c}$$

$$\bar{x}_f(\tau|t_k) \in \bar{\mathcal{X}}(\tau - t_k) \tag{33d}$$

$$\bar{p}_f^e(t_k + T|t_k) \in \mathcal{X}_f \tag{33e}$$

where $\tau \in [t_k, t_k + T]$, $\bar{\mathcal{U}} = \mathcal{U} \sim \mathscr{B}(\varrho)$, $\varrho \triangleq \max_{x\in\mathcal{X}} \|B^\dagger(x)B_w(x)\|\frac{\eta_1\|\psi\|\beta(\psi)}{c(\psi)}$ and $\bar{\mathcal{X}}(\tau - t_k) = \mathcal{X} \sim \mathcal{B}(\tau - t_k)$.

The cost function $J(\bar{p}_f^e(t_k), \bar{u}_f(\cdot), T)$ with prediction horizon T is defined by

$$J(\bar{p}_f^e(t_k), \bar{u}_f(\cdot), T) = \int_{t_k}^{t_k+T} F(\bar{p}_f^e(\tau|t_k), \bar{u}_f(\tau|t_k))d\tau + V_f(\bar{p}_f^e(t_k + T|t_k))$$

where the stage cost function $F(\bar{p}_f^e(\tau|t_k), \bar{u}_f(\tau|t_k)) = \|\bar{p}_f^e(\tau|t_k)\|_Q^2 + \|\bar{u}_f(\tau|t_k))\|_R^2$ and the terminal cost function $V_f(\bar{p}_f^e(t_k + T|t_k)) = \|\bar{p}_f^e(t_k + T|t_k)\|_P^2$. The weighting matrices are given by $Q = \text{diag}\{q_1, q_2\}$, $R = \text{diag}\{r_1, r_2\}$ and $P = \text{diag}\{1/2, 1/2\}$ with positive scalars q_i and r_i, $i = 1, 2$.

Corresponding to Assumption 4, the specified terminal controller $\kappa_f(\cdot)$ is given in Lemma 7.

Lemma 7 (see [35]): For nominal tracking error dynamics (30), if weighting parameters q_i and r_i are chosen such that there exist positive constants

$$\bar{\mu}_i \in \left(\frac{1 - \sqrt{1 - 4r_iq_i}}{2r_i}, \frac{1 + \sqrt{1 - 4r_iq_i}}{2r_i}\right),\ i = 1, 2$$

then there exists a region

$$\Omega \triangleq \left\{\bar{p}_f^e \mid \bar{\mu}_1\frac{|\bar{x}_{f,1}^e|}{a} + \bar{\mu}_2\frac{|\bar{x}_{f,2}^e|}{a} \leq 1 - \gamma\right\}$$

and terminal controller $\kappa_f(\cdot)$ in Ω

$$\kappa_f(\bar{p}_f^e) = \begin{bmatrix} \bar{\mu}_1\bar{x}_{f,1}^e + (v_r - d_y\omega_r)\cos\theta_{rf} - d_x\omega_r\sin\theta_{rf} \\ (\bar{\mu}_2\bar{x}_{f,2}^e + (v_r - d_y\omega_r)\sin\theta_{rf} + d_x\omega_r\cos\theta_{rf})/\rho \end{bmatrix}$$

such that, for all $\bar{p}_f^e(t) \in \Omega$ and $\tau \geq t$

$$\bar{p}_f^e(\tau) \in \Omega, \quad \kappa_f(\bar{p}_f^e(\tau)) \in \mathcal{U}$$
$$\dot{V}_f(\bar{p}_f^e(\tau)) + F(\bar{p}_f^e(\tau), \kappa_f(\bar{p}_f^e(\tau))) \leq 0. \tag{34}$$

D. Theoretical Analysis

Unlike the regulation problem discussed in Section III, a trajectory tracking problem is considered for the nonholonomic mobile robot, which has the following particularities.

1) The velocity u_r of the leader is required to be restricted (i.e., $\|u_r\| \leq \frac{a}{\sqrt{2}\|M\|}$) to ensure that the follower can catch up with the desired position d regarding the Frenet–Serret frame ${}^rO$ fixed on the leader.

2) The control input u_f of the follower is determined by taking into account the information from the leader, which induces the specialized terminal controller $\kappa_f(\cdot)$ in Lemma 7 and further influences the subsequent theoretical analysis.

3) The control objective is to control the first two dimensions of follower state x_f tracking the desired reference trajectory generated by the virtual point d, that is, driving the tracking error $p_f^e \to 0$.

Here, we simply list the theoretical results for the nonholonomic mobile robot tracking problem and provide a brief proof.

Theorem 4: For system (29), Problem 2 under the proposed DRMPC framework is recursively feasible for all sampling instants t_k, $k \in \mathbb{N}$, if Problem 2 is feasible at the initial time t_0 and the following conditions are satisfied:

$$\text{(i)}\ \frac{\varpi_m}{a}\left(e^{a\delta} - 1\right)e^{a(T-\delta)} \leq r - \varepsilon; \tag{35}$$

$$\text{(ii)}\ \bar{\mu}_{\min}\delta \geq ln\frac{r}{\varepsilon}; \tag{36}$$

$$\text{(iii)}\ \mathcal{X}_r \subseteq \mathcal{X} \sim \mathcal{B}(T); \tag{37}$$

where $r = \frac{a}{\sqrt{\mu_1^2+\mu_2^2}}\left(1-\varrho\frac{\sqrt{(a^2+b^2)}}{ab}-\gamma\right)$ and $\bar{\mu}_{\min} = \min\{\bar{\mu}_1, \bar{\mu}_2\}$.

Proof: The brief proof is shown in Appendix B.

Theorem 5: Under the proposed DRMPC framework, the resulting closed-loop system (32) is regional input-to-state practical stable, which implies the regional ISpS for system (29).

Remark 9: The conservativeness of the DRMPC framework mainly arises from the Lipschitz constant ℓ of nonlinear systems, the possibly maximal estimation of compensated disturbance and possible open-loop prediction behaviors over the prediction horizon considered in the theoretical analyses.

V. Simulation Results

Using MATLAB 2017a and ICLOCS toolbox, simulation comparisons are made with an MPC strategy without the disturbance compensation and the ISM-MPC algorithm (defined hereinafter). Consider the nonholonomic mobile robot dynamics (26) with

$$B_w(x_f) = \begin{bmatrix} \cos\theta_f & -\sin\theta_f \\ \sin\theta_f & \cos\theta_f \\ 0 & 0 \end{bmatrix}$$

where the disturbance $B_w(x_f)w(t)$ is mismatched and caused by the sideslip. The simulation parameters are introduced in [26]. The velocities of driving wheels are bounded with $a = 0.13\,\mathrm{m/s}$ and the wheel base is $\rho = 0.0267\,\mathrm{m}$. Thereby, $b = \frac{a}{\rho} = 4.8598\,\mathrm{rad/s}$ and the input constraint can be described by a diamond-shaped region $\mathcal{U} = \{[v_f, \omega_f]^\top \mid \frac{|v_f|}{0.13} + \frac{|\omega_f|}{4.8598} \le 1\}$. The state constraint set can be described by $\mathcal{X} = \{x_f = [x_{f,1}, x_{f,2}, \theta_f]^\top \mid -1 \le x_{f,1} \le 1, -1 \le x_{f,2} \le 0.85, -\pi < \theta_f \le \pi\}$. The initial position of the follower is set as $x_{f0} = [0.2, -0.2, -\frac{\pi}{2}]^\top$. The external disturbance $w(t) = [w_1(t), w_2(t)]^\top$ can be expressed as $w(t) = w_a(t)$ with

$$w_a(t) = \begin{bmatrix} 1 \\ 0.1 \end{bmatrix}(0.0154\sin(2.5t+1) + 0.0138\cos(1.25t))$$

which is bounded by $\eta_1 = 0.0289$ and its derivative is bounded by $\eta_2 = 0.0540$. For nonlinear observer (8), the nonlinear function $\phi(x_f)$ and observer gain $L(x_f)$ can be designed as

$$\phi(x_f) = L_1 \begin{bmatrix} x_{f,1}\cos\theta_f + x_{f,2}\sin\theta_f \\ -x_{f,1}\sin\theta_f + x_{f,2}\cos\theta_f \end{bmatrix}$$

$$L(x_f) = \frac{\partial\phi(x_f)}{\partial x_f} = L_1 \begin{bmatrix} \cos\theta_f & \sin\theta_f & -x_{f,1}\sin\theta_f + x_{f,2}\cos\theta_f \\ -\sin\theta_f & \cos\theta_f & -x_{f,1}\cos\theta_f - x_{f,2}\sin\theta_f \end{bmatrix}$$

with $L_1 = \mathrm{diag}\{10, 5\}$. For the optimization problem, the prediction horizon and the sampling interval are chosen as $T = 3\,\mathrm{s}$ and $\delta = 0.05\,\mathrm{s}$. The weighting matrices in the cost function are set as $Q = 0.06I_2$, $R = 0.002I_2$. The terminal parameters are chosen as $\bar{\mu}_1 = \bar{\mu}_2 = 1.5$ and $\varepsilon = 0.0482$. The tightened input constraint (33c) can be computed as $\bar{u}_f(\tau|t_k) \in \bar{\mathcal{U}} = \{[v_f, \omega_f]^\top \mid \frac{|v_f|}{a} + \frac{|\omega_f|}{b} \le 0.7770\}$.

The leader is designed to execute the uniform circling motion with initial position $x_r = [0, 0, \frac{\pi}{3}]^\top$, linear velocity $v_r = 0.025\,\mathrm{m/s}$ and angular velocity $w_r = 0.06\,\mathrm{rad/s}$. The desired tracking position is set as $d = [d_x, d_y]^\top = [-0.1, -0.1]^\top$ regarding the Frenet–Serret frame ${}^rO$ fixed on the mobile leader. The control objective is to keep the leader–follower formulation as shown in Fig. 2(b).

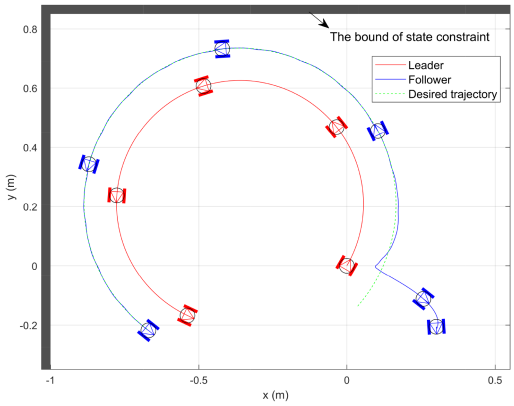

Fig. 3. State trajectory of the closed-loop system.

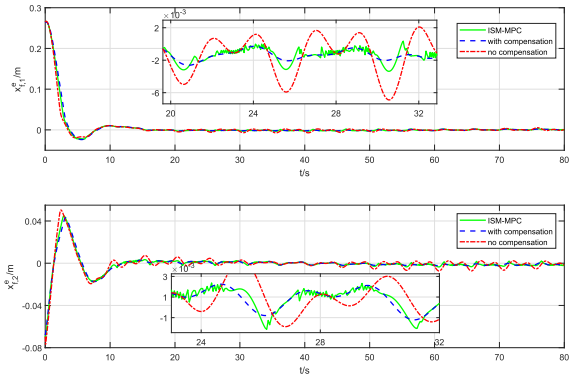

Fig. 4. Tracking error trajectory with/without compensation.

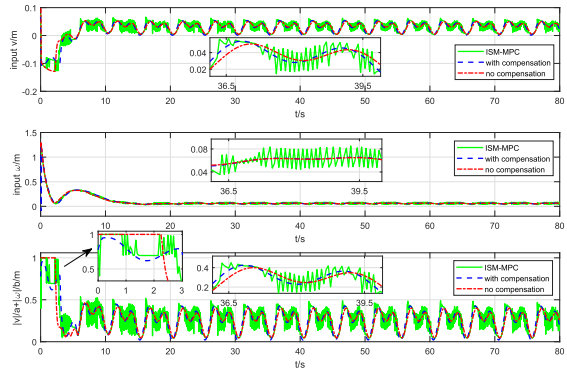

Fig. 5. Input trajectory with/without compensation.

The DRMPC framework is implemented and corresponding results are shown in Figs. 3–6. Fig. 3 illustrates the tracking task under the proposed algorithm and the leader–follower configuration is performed effectively, where the grey shading is the zone violating state constraint $\mathcal{X}$. The real-time tracking error p_f^e and control input u_f of the follower are shown in Figs. 4

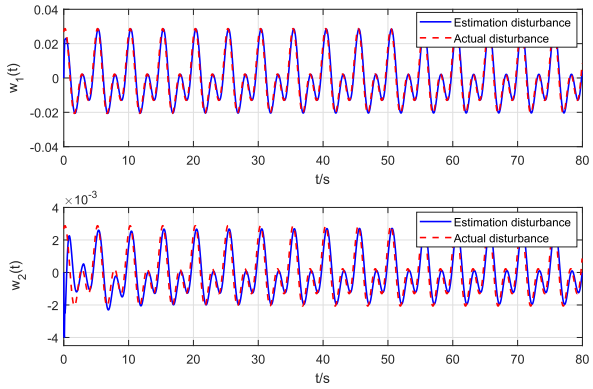

Fig. 6. Disturbance estimation performance.

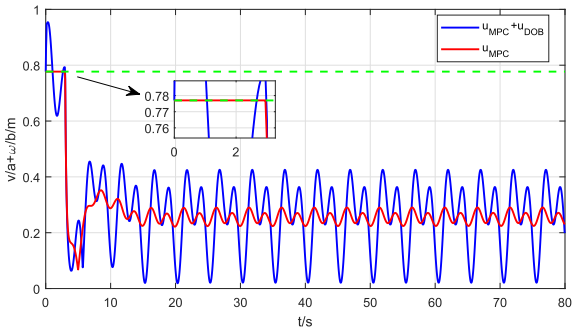

Fig. 7. Comparison between $u_f(t)$ and $u_{\mathrm{MPC}}(t)$.

and 5, respectively. The actual disturbance and the disturbance estimation under the designed observer are shown in Fig. 6.

1) *Comparison to an MPC control strategy without the disturbance compensation:* The strategy without the disturbance compensation is set as $u_{\mathrm{DOB}}(t) = -\hat{h}(t) = 0$ with $\bar{\mathcal{U}} = \mathcal{U}$ and $\varpi_m = \varpi(t_0, \infty) = \sup_{s\in[t_0,\infty)} \bar{B}_w \|w(s)\|$. It can be seen in Fig. 4 that the proposed algorithm effectively alleviates the negative effects of disturbances, while as shown in Fig. 5 the control input without the disturbance compensation is a bit delayed in response to disturbances.
2) *Comparison to the ISM-MPC algorithm:* Because the algorithm in [29] cannot be utilized directly for input-affine nonlinear system (1), we replace the sliding manifold in [29] by the sliding manifold in [39] and call the resulting algorithm "ISM-MPC." The gain of unit vector approach in [39] is set as $0.25\,\eta_1$. It can be seen in Figs. 4 and 5 that the DRMPC framework achieves a better disturbance compensation compared with ISM-MPC and there exists inevitable chattering when adopting the sliding mode approach in ISM-MPC.

As mentioned in Section III, the optimal control input $u_{\mathrm{MPC}}(t)$ mainly focuses on the control performance and the disturbance compensation input $u_{\mathrm{DOB}}(t)$ is in charge of the disturbance rejection. To further highlight the effect of the disturbance compensation under the DRMPC framework, we compare the overall control input $u_f(t) = u_{\mathrm{MPC}}(t) + u_{\mathrm{DOB}}(t)$

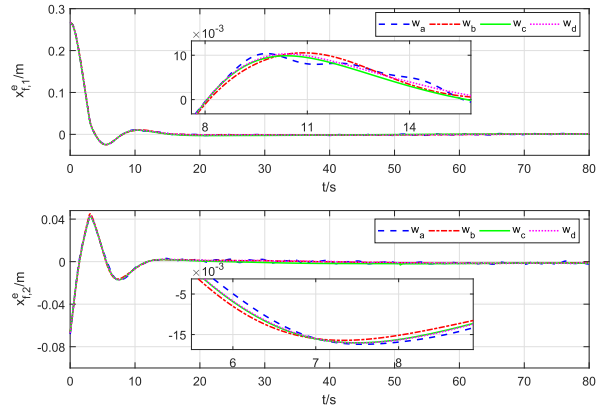

Fig. 8. Tracking error trajectories under different classes of disturbances.

with the optimal control input $u_{\mathrm{MPC}}(t)$ in Fig. 7. Specifically, in Fig. 7, the input $u_{\mathrm{MPC}}(t)$ reaches its maximal bound of input constraint $u_{\mathrm{MPC}}(t) \in \bar{\mathcal{U}} = \{[v_f, \omega_f]^\top \mid \frac{|v_f|}{a} + \frac{|\omega_f|}{b} \leq 0.7770\}$. The whole input $u_f(t)$ does not activate the physical input constraint $u_f(t) \in \mathcal{U} = \{[v_f, \omega_f]^\top \mid \frac{|v_f|}{a} + \frac{|\omega_f|}{b} \leq 1\}$. The tightened input constraint set $\bar{\mathcal{U}} = \{[v_f, \omega_f]^\top \mid \frac{|v_f|}{a} + \frac{|\omega_f|}{b} \leq 0.7770\}$ is obtained by taking into account the upper bound of $\|u_{\mathrm{DOB}}(t)\|$, and its conservativeness is discussed in Remark 9.

The proposed DRMPC framework is also verified compatibly to more general classes of disturbances satisfying Assumption 1 in Fig 8. Here, additional three classes of disturbances are considered. The disturbance $w_b(t) = \begin{bmatrix} 1 \\ 0.1 \end{bmatrix} \cdot 0.0288 \sin\left(\frac{\pi}{3} \cdot t\right) e^{-\frac{t}{10}}$ denotes the vanishing disturbance extracted from [13] and the disturbance $w_c(t) = \begin{bmatrix} 1 \\ 0.1 \end{bmatrix} \cdot 0.0144(x_{f,1}x_{f,2}^2 + \sin(x_{f,2}))$ depends on the system state $x_f(t)$ explicitly as in [40]. The disturbance $w_d(t)$ is generated by the *smoothing splines* [41] stochastically sampling from $\left\{ \begin{bmatrix} 1 \\ 0.1 \end{bmatrix} w \mid \|w\| \leq 0.0144 \right\}$. As shown in Fig. 8, the leader–follower configuration is effectively achieved with only slight differences under these four classes of disturbances. The variants of these disturbances are widely used in the family of the nonlinear control, which implies the extensive applicability of the proposed DRMPC framework.

VI. Conclusion

In this article, a DRMPC framework is developed for a group of input-affine nonlinear systems subject to constraints and state-dependent disturbances. The approach exploits the disturbance estimation information from the disturbance observer and the space decomposition method to achieve the matched disturbance compensation. Under the disturbance compensation input, the resulting system is then used to calculate the optimal control input with the aim of system performance improvement. The theoretical properties including recursive feasibility and regional input-to-state practical stability are guaranteed. The proposed framework is also applicable to the tracking

problem of the nonholonomic mobile robot. Simulation results reveal that this approach outperforms the corresponding robust MPC method without disturbance observer in terms of control performance.

APPENDIX A
PRELIMINARY LEMMAS

The following lemmas are useful for the main proofs in Appendix B.

Lemma 8 ([42]): The norm of matrix exponential for a Hurwitz matrix $A \in \mathbb{R}^{n\times n}$ is bounded by $\|e^{At}\| \le \beta(A)e^{-c(A)t}$, $t \ge 0$, where $\beta(A) \triangleq \sqrt{\|Y^{-1}\|\|Y\|}$, $c(A) \triangleq 1/(2\|Y\|)$ and Y is the unique Hermitian matrix obtained by solving the Lyapunov equation $YA + A^\top Y = -I$.

Lemma 9: The remainder term $\hat{g}(t)$ in (17) satisfies

$$\|\hat{g}(t)\| \le \|B_w(x)\hat{w}(t)\| \tag{38}$$

with $\hat{g}(t) = U_2(x)U_2^\top(x)B_w(x)\hat{w}(t) = U_2(x)U_2^\dagger(x)B_w(x)\hat{w}(t)$.

Proof: The proof is given for nontrivial cases $\mathscr{G} \neq \{\mathbf{0}\}$. For any x, let matrix $A(x)$ belong to a set of matrices $\{U_1(x)U_1^\top(x), U_2(x)U_2^\top(x), B(x)B^\dagger(x), U_2(x)U_2^\dagger(x)\}$, then $A^\top(x)A(x) = A(x)$ holds. Take λ_a, v_a as an eigenvalue and the corresponding eigenvector of $A(x)$. Then

$$A(x)v_a = \lambda_a v_a \Rightarrow v_a^\top A^\top(x)A(x)v_a = \lambda_a^2\|v_a\|^2. \tag{39}$$

It follows from $A^\top(x)A(x) = A(x)$ that

$$v_a^\top A^\top(x)A(x)v_a = v_a^\top A(x)v_a = \lambda_a\|v_a\|^2. \tag{40}$$

Equation (39) together with (40) implies $\lambda_a = 0$ or $\lambda_a = 1$ and $\operatorname{rank}(A(x)) < n$ for all $A(x) \in \{U_1(x)U_1^\top(x), U_2(x)U_2^\top(x), B(x)B^\dagger(x), U_2(x)U_2^\dagger(x)\}$.

Due to $U_1(x)U_1^\top(x) + U_2(x)U_2^\top(x) = B(x)B^\dagger(x) + U_2(x)U_2^\dagger(x) = I_{n\times n}$, the rank of $A(x)$ cannot be zero. Therefore, the maximum eigenvalue of $A(x)$ is one and $\|A(x)\| = 1$ for any x. By the norm compatibility

$$\begin{aligned}\|\hat{g}(t)\| &= \left\|U_2(x)U_2^\top(x)B_w(x)\hat{w}(t)\right\| \\ &\le \left\|U_2(x)U_2^\top(x)\right\|\|B_w(x)\hat{w}(t)\| \\ &= \|B_w(x)\hat{w}(t)\|\end{aligned}$$

which completes the proof.

Lemma 10 (Gronwall inequality): Let $\mathscr{I}$ denote an interval of the real line of the form $[a,\infty)$ or $[a,b]$ or $[a,b)$ with $a < b$. Let $\alpha(\cdot)$, $\beta(\cdot)$ and $u(\cdot)$ be real-valued functions defined on $\mathscr{I}$. Assume that $\beta(\cdot)$ and $u(\cdot)$ are continuous and that the negative part of $\alpha(\cdot)$ is integrable on every closed and bounded subinterval of $\mathscr{I}$. If $\beta(\cdot)$ is nonnegative and if $u(\cdot)$ satisfies the integral inequality

$$u(t) \le \alpha(t) + \int_a^t \beta(s)u(s)ds \qquad \forall t \in \mathscr{I}$$

then

$$u(t) \le \alpha(t) + \int_a^t \alpha(s)\beta(s)\exp\left(\int_s^t \beta(r)dr\right)ds \qquad \forall t \in \mathscr{I}.$$

Further, if $\alpha(\cdot)$ can be decomposed as $\alpha(\cdot) = \gamma_1(\cdot)\cdot\gamma_2(\cdot)$, where $\gamma_1(\cdot)$, $\gamma_2(\cdot)$ are both real-valued functions and γ_1 is nondecreasing, then

$$u(t) \le \gamma_1(t)\left[\gamma_2(t) + \int_a^t \gamma_2(s)\beta(s)\exp\left(\int_s^t \beta(r)dr\right)ds\right] \qquad \forall t \in \mathscr{I}. \tag{41}$$

In particular, if $\alpha(\cdot)$ is a constant α, then

$$u(t) \le \alpha\exp\left(\int_a^t \beta(s)ds\right) \qquad \forall t \in \mathscr{I}. \tag{42}$$

APPENDIX B
MAIN PROOFS

A. Proof of Theorem 2

Proof: To show the recursive feasibility, we need to prove the feasible region of optimal control problem (18) is nonempty at time $t_{k+1} = t_k + \delta$ if the optimal control problem is feasible at time t_k, $k \in \mathbb{N}$. To this end, the following candidate solution at time t_{k+1} is constructed:

$$\tilde{u}(\tau|t_{k+1}) = \begin{cases}\bar{u}^*(\tau|t_k), & \tau \in [t_{k+1}, t_k+T) \\ \kappa_f(\tilde{x}(\tau|t_{k+1})), & \tau \in [t_k+T, t_{k+1}+T).\end{cases} \tag{43}$$

The proof is divided into three parts.

Part 1: Show that the state trajectory $\tilde{x}(\tau|t_{k+1})$ corresponding to (43) can enter terminal region $\mathscr{X}_f$ at time $\tau = t_{k+1} + T$, i.e., $\tilde{x}(t_{k+1}+T|t_{k+1}) \in \mathscr{X}_f$ in (18e), where the trajectory $\tilde{x}(\tau|t_{k+1})$ is generated by

$$\dot{\tilde{x}}(\tau|t_{k+1}) = f(\tilde{x}) + B(\tilde{x})\tilde{u}(\tau|t_{k+1}).$$

The difference between state trajectory $\tilde{x}(\tau|t_{k+1})$ and optimal state trajectory $\bar{x}^*(\tau|t_k)$ can be upper bounded, for all $\tau \in [t_{k+1}, t_k+T]$, by

$$\begin{aligned}&\|\tilde{x}(\tau|t_{k+1}) - \bar{x}^*(\tau|t_k)\| \\ &= \|x(t_{k+1}) + \int_{t_{k+1}}^{\tau} \mathscr{F}(\tilde{x}(s|t_{k+1}), \bar{u}^*(s|t_k))ds \\ &\quad - \bar{x}^*(t_{k+1}|t_k) - \int_{t_{k+1}}^{\tau} \mathscr{F}(\bar{x}^*(s|t_k), \bar{u}^*(s|t_k))ds\| \\ &\overset{(20)}{\le} \frac{\varpi(t_k, t_{k+1})}{\ell}\left(e^{\ell\delta} - 1\right) + \ell\int_{t_{k+1}}^{\tau}\|\tilde{x}(s|t_{k+1}) - \bar{x}^*(s|t_k)\|ds \\ &\overset{(42)}{\le} \frac{\varpi(t_k, t_{k+1})}{\ell}\left(e^{\ell\delta} - 1\right)e^{\ell(\tau - t_{k+1})}.\end{aligned} \tag{44}$$

Substituting $\tau = t_k + T$ into (44), we have

$$\begin{aligned}&\|\tilde{x}(t_k+T|t_{k+1}) - \bar{x}^*(t_k+T|t_k)\|_P \\ &\le \bar{\lambda}(\sqrt{P})\frac{\varpi(t_k, t_{k+1})}{\ell}\left(e^{\ell\delta} - 1\right)e^{\ell(T-\delta)}.\end{aligned}$$

It follows from the triangle inequality that

$$\begin{aligned}&\|\tilde{x}(t_k+T|t_{k+1})\|_P \\ &\le \|\bar{x}^*(t_k+T|t_k)\|_P + \bar{\lambda}(\sqrt{P})\frac{\varpi(t_k, t_{k+1})}{\ell}\left(e^{\ell\delta} - 1\right)e^{\ell(T-\delta)} \\ &\overset{(21)}{\le} \varepsilon + (r - \varepsilon) \\ &= r.\end{aligned} \tag{45}$$

This implies that the state $\tilde{x}(t_k+T|t_{k+1})$ enters the nominal terminal region $\mathcal{X}_r$ and the controller switches to terminal controller $\kappa_f(\cdot)$ at prediction time t_k+T.

According to Assumption 4, for $\tau\in[t_k+T,t_{k+1}+T]$

$$\dot{V}_f(\tilde{x}(\tau|t_{k+1}))\overset{(19)}{\leq}$$
$$-F(\tilde{x}(\tau|t_{k+1}),\tilde{u}(\tau|t_{k+1}))\leq-\|\tilde{x}(\tau|t_{k+1})\|_{Q^*}^2$$

with $Q^*=Q+K^\top RK$. Further

$$\dot{V}_f(\tilde{x}(\tau|t_{k+1}))\leq-\frac{\underline{\lambda}(Q^*)}{\overline{\lambda}(P)}V_f(\tilde{x}(\tau|t_{k+1})).$$

By comparison principle [43], we have

$$V_f(\tilde{x}(\tau|t_{k+1}))\leq V_f(\tilde{x}(t_k+T|t_{k+1}))e^{-\frac{\underline{\lambda}(Q^*)}{\overline{\lambda}(P)}(\tau-t_k-T)}.$$

Substitute $\tau=t_{k+1}+T$ and the above equation can be equivalently written as

$$\|\tilde{x}(t_{k+1}+T|t_{k+1})\|_P\leq\|\tilde{x}(t_k+T|t_{k+1})\|_P e^{-\frac{\underline{\lambda}(Q^*)}{2\overline{\lambda}(P)}\delta}.$$

Due to $\|\tilde{x}(t_k+T|t_{k+1})\|_P\leq r$ and the condition (ii) $\frac{\underline{\lambda}(Q^*)\delta}{2\overline{\lambda}(P)}\geq\ln\frac{r}{\varepsilon}$, we obtain

$$\|\tilde{x}(t_{k+1}+T|t_{k+1})\|_P\leq\varepsilon$$

implying the satisfaction of terminal constraint $\tilde{x}(t_{k+1}+T|t_{k+1})\in\mathcal{X}_f$.

Part 2: Show that the candidate solution (43) satisfies input constraint (18c) at time t_{k+1}.

For $\tau\in[t_{k+1},t_k+T)$, the candidate input $\tilde{u}(\tau|t_{k+1})$ is equal to optimal input $\bar{u}^*(\tau|t_k)$, which satisfies the input constraint (18c) trivially.

From Assumption 4 and the fact $\tilde{x}(t_k+T|t_{k+1})\in\mathcal{X}_r$, it follows that, for $\tau\in[t_k+T,t_{k+1}+T]$, the terminal controller $\kappa_f(\tilde{x}(\tau|t_{k+1}))$ is adopted and $\tilde{x}(\tau|t_{k+1})$ remains in $\mathcal{X}_r$, which further implies the satisfaction of input constraint (18c).

Part 3: Show that the state trajectory under (43) satisfies state constraint (18d), i.e., $\tilde{x}(\tau|t_{k+1})\in\bar{\mathcal{X}}(\tau-t_{k+1})$.

For $\tau\in[t_{k+1},t_k+T)$, take $x=\bar{x}^*(\tau|t_k)$, $y=\tilde{x}(\tau|t_{k+1})$ in Lemma 4. Because of $\|\tilde{x}(\tau|t_{k+1})-\bar{x}^*(\tau|t_k)\|\leq\frac{\varpi_m}{\ell}(e^{\ell\delta}-1)e^{\ell(\tau-t_{k+1})}$, it holds $\tilde{x}(\tau|t_{k+1})\in\mathcal{X}\sim\mathcal{B}(\tau-t_{k+1})$.

Consider $\tau\in[t_k+T,t_{k+1}+T]$. According to Assumption 4, $\mathcal{X}_r$ is a positive invariant set under controller $\kappa_f(\cdot)$. Therefore, if condition (iii) $\mathcal{X}_r\subseteq\mathcal{X}\sim\mathcal{B}(T)$ is satisfied, then $\tilde{x}(\tau|t_{k+1})\in\mathcal{X}_r\subseteq\mathcal{X}\sim\mathcal{B}(T)\subseteq\mathcal{X}\sim\mathcal{B}(\tau-t_{k+1})$.

It can be concluded that (43) is a feasible solution at time t_{k+1}. By induction, recursive feasibility is ensured by implementing the DRMPC framework.

B. Proof of Theorem 3

For $t\in[t_k,t_{k+1})$, define Lyapunov function candidate as

$$V(t,x(t))\triangleq\int_t^{t_{k+1}+T_\delta}F(\tilde{x}^*(\tau|t),\tilde{u}^*(\tau|t))d\tau+V_f(\tilde{x}^*(t_{k+1}+T_\delta|t)) \tag{46}$$

where $T_\delta\triangleq T-\delta$ and $\tilde{u}^*(\tau|t)\triangleq\bar{u}^*(\tau|t_k)$ for all $\tau\in[t,t_{k+1}+T_\delta)$. The state $\tilde{x}^*(\tau|t)$ is generated by

$$\dot{\tilde{x}}^*(\tau|t)=f(\tilde{x}^*)+B(\tilde{x}^*)\tilde{u}^*(\tau|t)$$

with initial state $\tilde{x}^*(t|t)\triangleq x(t)$.

Step 1: Find a $\mathcal{K}_\infty$ function $\alpha_1(\|x(t)\|)$ in (3) as the lower bound on $V(t,x(t))$.

From (46)

$$\begin{aligned}V(t,x(t))&=\int_t^{t_{k+1}+T_\delta}F(\tilde{x}^*(\tau|t),\tilde{u}^*(\tau|t))d\tau\\&\quad+V_f(\tilde{x}^*(t_{k+1}+T_\delta|t))\\&\geq\underline{\lambda}(Q)\int_t^{t_{k+1}+T_\delta}\|\tilde{x}^*(\tau|t)\|^2d\tau\\&\geq\underline{\lambda}(Q)\int_0^{T^*}(\|x(t)\|-s\varphi)^2ds\end{aligned} \tag{47}$$

where $\varphi\triangleq\sup_{x\in\mathcal{X},u\in\mathcal{U},w\in\mathcal{W}}\|\mathscr{F}(x,u)+B_w(x)w\|$ is the maximum derivative of the evolution of system (1) and

$$T^*\triangleq\begin{cases}\frac{\|x(t)\|}{\varphi}, & \|x(t)\|\leq T_\delta\varphi\\ T_\delta, & \|x(t)\|>T_\delta\varphi.\end{cases}$$

The last inequality (47) states that the lower bound of $V(t,x(t))$ can be obtained by driving the state $x(t)$ to the origin at full speed and shrinking the integral interval. Furthermore, when $\|x(t)\|\leq T_\delta\varphi$

$$\underline{\lambda}(Q)\int_0^{T^*}(\|x(t)\|-s\varphi)^2ds=\underline{\lambda}(Q)\frac{\|x(t)\|^3}{3\varphi} \tag{48}$$

and when $x(t)>T_\delta\varphi$

$$\begin{aligned}&\underline{\lambda}(Q)\int_0^{T^*}(\|x(t)\|-s\varphi)^2ds\\&=\underline{\lambda}(Q)\left(\frac{\varphi^2(T^*)^3}{3}-\varphi(T^*)^2\|x(t)\|+T^*\|x(t)\|^2\right).\end{aligned} \tag{49}$$

Consider (48) and (49) together and construct a function $\alpha_1(\cdot):\mathbb{R}\to\mathbb{R}$ as

$$\alpha_1(\|x(t)\|)\triangleq\begin{cases}\underline{\lambda}(Q)\frac{\|x(t)\|^3}{3\varphi}, & \|x(t)\|\leq T_\delta\varphi\\ \underline{\lambda}(Q)\left(\frac{\varphi^2(T^*)^3}{3}+T^*\|x(t)\|^2\right.\\ \qquad\left.-\varphi(T^*)^2\|x(t)\|\right), & \|x(t)\|>T_\delta\varphi\end{cases}$$

which is continuous, positive definite, and strictly increasing with respect to $\|x(t)\|$. Clearly when $\|x(t)\|\to\infty$, it holds $\alpha_1(\|x(t)\|)\to\infty$. Hence $\alpha_1(\|x(t)\|)$ is an appropriate $\mathcal{K}_\infty$ function satisfying condition (3).

Step 2: Find a $\mathcal{K}_\infty$ function $\alpha_2(\|x(t)\|)$ and a positive constant c_1 in (4) as the upper bound on $V(t,x(t))$.

For the case of $x(t)\in\mathcal{X}_r$

$$\begin{aligned}V(t,x(t))=&\int_0^{T_\delta+a_\delta}\|\tilde{x}^*(t+s|t)\|_Q^2+\|\tilde{u}^*(t+s|t)\|_R^2ds\\&+\|\tilde{x}^*(t_{k+1}+T_\delta|t)\|_P^2\end{aligned}$$

where $a_\delta=t_{k+1}-t\in[0,\delta)$. Then

$$\begin{aligned}V(t,x(t))\leq&\ \overline{\lambda}(Q^*)\int_0^T(\|x(t)\|+s\varphi)^2ds\\&+\overline{\lambda}(P)(\|x(t)\|+T\varphi)^2\\\leq&\ \overline{\lambda}(Q^*)(T\|x(t)\|^2+T^2\varphi\|x(t)\|)\end{aligned}$$

$$+\overline{\lambda}(P)(\|x(t)\|^2+2T\varphi\|x(t)\|)+\overline{\lambda}(Q^*)\frac{T^3\varphi^2}{3}+\overline{\lambda}(P)T^2\varphi^2.$$

Defining $\tilde{\alpha}_2(\|x(t)\|)=\overline{\lambda}(Q^*)(T\|x(t)\|^2+T^2\varphi\|x(t)\|)+\overline{\lambda}(P)(\|x(t)\|^2+2T\varphi\|x(t)\|)$ and $c_1=\overline{\lambda}(Q^*)\frac{T^3\varphi^2}{3}+\overline{\lambda}(P)T^2\varphi^2$, we have

$$V(t,x(t))\le\tilde{\alpha}_2(\|x(t)\|)+c_1,\ \forall x(t)\in\mathcal{X}_r.$$

For the case of $x(t)\in\Psi$, the compactness of $\mathcal{X}$ and $\mathcal{U}$ implies that the function $V(t,x(t))$ is bounded by a constant $\bar{J}$, i.e. $V(t,x(t))\le\bar{J}$. Defining $\bar{r}\triangleq\max(1,\frac{\bar{J}}{\tilde{\alpha}_2(\check{r})})$ and $\alpha_2(\|x(t)\|)\triangleq\bar{r}\tilde{\alpha}_2(\|x(t)\|)$, it follows that $\alpha_2(\|x(t)\|)\ge\tilde{\alpha}_2(\|x(t)\|)$ and

$$V(t,x(t))\le\alpha_2(\|x(t)\|)+c_1,\ \forall x(t)\in\mathcal{X}_r. \tag{50}$$

The nominal terminal region $\mathcal{X}_r$ is nonempty and there exists $\check{r}>0$ such that $\mathscr{B}(\check{r})\subseteq\mathcal{X}_r$. Therefore, for all $x(t)\in\Psi/\mathcal{X}_r$, it holds that $\tilde{\alpha}_2(\|x(t)\|)>\tilde{\alpha}_2(\check{r})$ and

$$V(t,x(t))\le\bar{J}\le\bar{J}\frac{\tilde{\alpha}_2(\|x(t)\|)}{\tilde{\alpha}_2(\check{r})}\le\alpha_2(\|x(t)\|)+c_1. \tag{51}$$

Inequality (50) together with (51) ensures the satisfaction of condition (4).

Step 3: Show that $V(t,x(t))$ satisfies condition (5) on continuous points and condition (6) when condition (5) does not hold.

For the continuous part of function $V(t,x(t))$, i.e., $t\in[t_k,t_{k+1})$

$$\dot{V}(t,x(t))\triangleq\lim_{h\to0^+}\frac{V(t+h,x(t+h))-V(t,x(t))}{h} \tag{52}$$

where h is sufficiently small such that $t+h\le t_{k+1}$. The numerator of (52) can be expressed as the sum of three terms

$$V(t+h,x(t+h))-V(t,x(t))=\Delta_1+\Delta_2+\Delta_3$$

where

$$\Delta_1\triangleq\int_{t+h}^{t_{k+1}+T_\delta}\|\tilde{x}^*(\tau|t+h)\|_Q^2-\|\tilde{x}^*(\tau|t)\|_Q^2d\tau$$

$$\Delta_2\triangleq\|\tilde{x}^*(t_{k+1}+T_\delta|t+h)\|_P^2-\|\tilde{x}^*(t_{k+1}+T_\delta|t)\|_P^2$$

$$\Delta_3\triangleq-\int_t^{t+h}\|\tilde{x}^*(\tau|t)\|_Q^2+\|\tilde{u}^*(\tau|t)\|_R^2d\tau.$$

Define $\varpi_h\triangleq\varpi(t,t+h)$, $\varpi_0\triangleq\varpi(t,t)$ and $\zeta(h)\triangleq\frac{\varpi_h}{\ell}(e^{\ell h}-1)$. For Δ_1, its upper bound is derived by

$$\begin{aligned}\Delta_1&\le\overline{\lambda}(Q)\int_{t+h}^{t_{k+1}+T_\delta}(\|\tilde{x}^*(\tau|t+h)-\tilde{x}^*(\tau|t)\|)\\&\quad\times(\|\tilde{x}^*(\tau|t+h)\|+\|\tilde{x}^*(\tau|t)\|)d\tau\\&\le\overline{\lambda}(Q)\int_{t+h}^{t_{k+1}+T_\delta}\zeta^2(h)e^{2\ell(\tau-t-h)}\\&\quad+2\|\tilde{x}^*(\tau|t)\|\zeta(h)e^{\ell(\tau-t-h)}d\tau\\&\le\overline{\lambda}(Q)\int_{t+h}^{t_{k+1}+T_\delta}\zeta^2(h)e^{2\ell(\tau-t-h)}\\&\quad+2\left(\frac{r}{\underline{\lambda}(\sqrt{P})}+\varphi(t_{k+1}+T_\delta-\tau)\right)\zeta(h)e^{\ell(\tau-t-h)}d\tau\\&\le\overline{\lambda}(Q)\Big\{\frac{\zeta^2(h)}{2\ell}(e^{2\ell(T_\delta+a_\delta-h)}-1)\\&\quad+2\frac{\zeta(h)}{\ell}\Big[\left(\frac{r}{\underline{\lambda}(\sqrt{P})}+\varphi(T_\delta+a_\delta-h)\right)(e^{\ell(T_\delta+a_\delta-h)}-1)\\&\quad-\varphi\left(\left(T_\delta+a_\delta-h-\frac{1}{\ell}\right)e^{\ell(T_\delta+a_\delta-h)}+\frac{1}{\ell}\right)\Big]\Big\}\\&\triangleq\overline{\Delta}_1\end{aligned}$$

where the second inequality can be obtained by determining the upper bound of $\|\tilde{x}^*(\tau|t+h)-\tilde{x}^*(\tau|t)\|$ analogous to (44) and the third inequality follows from $\|\tilde{x}^*(\tau|t)\|\le\|\tilde{x}^*(t_{k+1}+T_\delta|t)\|+\varphi(t_{k+1}+T_\delta-\tau)$. For Δ_2, the upper bound on it is obtained by

$$\begin{aligned}\Delta_2&=\|\tilde{x}^*(t_{k+1}+T_\delta|t+h)\|_P^2-\|\tilde{x}^*(t_{k+1}+T_\delta|t)\|_P^2\\&\le\Big[\|\tilde{x}^*(t_{k+1}+T_\delta|t+h)-\tilde{x}^*(t_{k+1}+T_\delta|t)\|_P\\&\quad\times(\|\tilde{x}^*(t_{k+1}+T_\delta|t+h)\|_P+\|\tilde{x}^*(t_{k+1}+T_\delta|t)\|_P)\Big]\\&\le2r\zeta(h)e^{\ell(T_\delta+a_\delta-h)}\triangleq\overline{\Delta}_2.\end{aligned}$$

For Δ_3, we have

$$\begin{aligned}\Delta_3&\le-\underline{\lambda}(Q)\int_0^{t^*}(\|x(t)\|-\varphi s)^2ds\\&=\begin{cases}-\underline{\lambda}(Q)\frac{\|x(t)\|^3}{3\varphi}, & \|x(t)\|\le h\varphi\\ \underline{\lambda}(Q)(-h\|x(t)\|^2\\ +\varphi h^2\|x(t)\|-\frac{\varphi^2h^3}{3}), & \|x(t)\|>h\varphi\end{cases}\\&\triangleq\overline{\Delta}_3\end{aligned}$$

with

$$t^*\triangleq\begin{cases}\frac{\|x(t)\|}{\varphi}, & \|x(t)\|\le h\varphi\\ h, & \|x(t)\|>h\varphi.\end{cases}$$

By letting $h\to0^+$, the limitations on $\frac{\Delta_i}{h}$, $i=1,2,3$ are given as

$$\lim_{h\to0^+}\frac{\overline{\Delta}_1}{h}=\varpi_0\psi_1$$

$$\lim_{h\to0^+}\frac{\overline{\Delta}_2}{h}=\varpi_0\psi_2$$

$$\lim_{h\to0^+}\frac{\overline{\Delta}_3}{h}=-\underline{\lambda}(Q)\|x(t)\|^2$$

where $\psi_1\triangleq\frac{2\overline{\lambda}(Q)}{\ell}[(\frac{r}{\underline{\lambda}(\sqrt{P})}+\varphi(T_\delta+a_\delta))(e^{\ell(T_\delta+a_\delta)}-1)-\varphi((T_\delta+a_\delta-\frac{1}{\ell})e^{\ell(T_\delta+a_\delta)}+\frac{1}{\ell})]$, $\psi_2\triangleq2re^{\ell(T_\delta+a_\delta)}$.

In view of the satisfaction of (10), the error system (9) is input-to-state stable. Therefore, there exists a $\mathcal{KL}_\infty$ function $\beta_1(\cdot,\cdot)$ and $\mathcal{K}$ functions $\sigma_1(\cdot)$, $\sigma_\beta(\cdot)$ such that $\|w_s(t)\|\le\beta_1(\eta_1,t)+\sigma_1(\eta_2)\le\beta_1(\eta_1,0)+\sigma_1(\eta_2)\le\sigma_\beta(\eta_1)+\sigma_1(\eta_2)$. Analogously, there exists a $\mathcal{KL}_\infty$ function $\beta_2(\cdot,\cdot)$ and a class $\mathcal{K}$ function $\sigma_2(\cdot)$ such that $\|\hat{w}(t)\|\le\beta_2(\|\hat{w}(t_0)\|,t)+\sigma_2(\|\eta_1\|)\le\sigma_2(\eta_1)$. Define $\sigma_3\triangleq\sigma_\beta+\sigma_2$ as

a new $\mathcal{K}$ function and

$$\alpha_3(\|x(t)\|) = \underline{\lambda}(Q)\|x(t)\|^2$$
$$\gamma(\|\mathbf{w}\|) = \varpi_{\sigma_3}(\psi_1+\psi_2)$$
$$c_2 = \varpi_{\sigma_1}(\psi_1+\psi_2)$$

where $\varpi_{\sigma_3} \triangleq \bar{B}_w\sigma_3(\eta_1)$, $\varpi_{\sigma_1} \triangleq \bar{B}_w\sigma_1(\eta_2)$ and $\varpi_{\sigma_3}+\varpi_{\sigma_1} \geq \varpi_m \geq \varpi_0$. Therefore, the continuous part of function $V(t,x(t))$ satisfies condition (5).

Consider the sampling instants t_{k+1} for $V(t,x(t))$, $k\in\mathbb{N}$. It holds that $x(t_{k+1}^-) = x(t_{k+1}^+) = x(t_{k+1})$ due to the continuity of the evolution on system state. Then, it follows from (46) that

$$\begin{aligned}
&V(t_{k+1}^+, x(t_{k+1}^+))\\
&= V(t_{k+1}, x(t_{k+1}))\\
&\leq V(t_{k+1}^-, x(t_{k+1}^-)) - V_f(\widehat{x}(t_{k+1}+T_\delta|t_{k+1}+T_\delta))\\
&\quad + V_f(\widehat{x}(t_{k+1}+T|t_{k+1}+T_\delta))\\
&\quad + \int_{t_{k+1}+T_\delta}^{t_{k+1}+T} F\left(\widehat{x}(\tau|t_{k+1}+T_\delta), \kappa_f(\widehat{x}(\tau|t_{k+1}+T_\delta))\right)d\tau
\end{aligned}$$

where $\widehat{x}(t_{k+1}+T_\delta|t_{k+1}+T_\delta) \triangleq \tilde{x}^*(t_{k+1}+T_\delta|t_{k+1}^-)$ and $\widehat{x}(\tau|t_{k+1}+T_\delta)$ is generated, for $\tau\in[t_{k+1}+T_\delta, t_{k+1}+T]$, by

$$\dot{\widehat{x}}(\tau|t_{k+1}+T_\delta) = f(\widehat{x}) + B(\widehat{x})\kappa_f(\widehat{x}).$$

Further, Assumption 4 implies that

$$\begin{aligned}
&V_f(\widehat{x}(t_{k+1}+T|t_{k+1}+T_\delta)) - V_f(\widehat{x}(t_{k+1}+T_\delta|t_{k+1}+T_\delta))\\
&+\int_{t_{k+1}+T_\delta}^{t_{k+1}+T} F\left(\widehat{x}(\tau|t_{k+1}+T_\delta), \kappa_f(\widehat{x}(\tau|t_{k+1}+T_\delta))\right)d\tau \leq 0.
\end{aligned}$$

Therefore, it holds that

$$V(t_{k+1}^+, x(t_{k+1}^+)) \leq V(t_{k+1}^-, x(t_{k+1}^-))$$

satisfying condition (6).

As for C2 in Definition 3, it is necessary to claim that the stable region Θ_w in (7) belongs to the attraction of region Ψ. There exists the same requirements for both ISS and regional ISpS. However, in the existing works, one usually avoids estimating Θ_w [29], [44] or omits the assertion [45]–[50] due to the difficulty in the calculation of the attraction of region Ψ and the conservativeness in the estimation of Θ_w for nonlinear systems. To make theory complete, similar with other related works, we default the satisfaction of C2.

C. Proof of Theorem 4

The feasible solution at time t_{k+1} is constructed as before

$$\tilde{u}(\tau|t_{k+1}) = \begin{cases} \bar{u}^*(\tau|t_k), & \tau\in[t_{k+1}, t_k+T)\\ \kappa_f(\tilde{x}(\tau|t_{k+1})), & \tau\in[t_k+T, t_{k+1}+T). \end{cases} \quad (53)$$

Main proofs can be derived by following the similar lines in the proof of Theorems 2 and 3. Here, we mainly emphasize the differences resulting from the specialized form of nominal terminal region $\mathbb{X}_r$ and terminal controller $\kappa_f(\cdot)$.

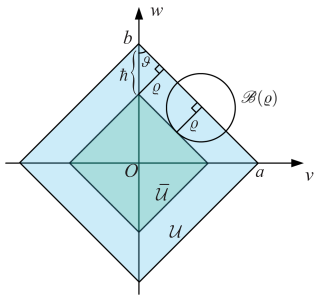

Fig. B1. Tightened input constraint set $\bar{\mathcal{U}}$.

(i) The nominal terminal region $\mathbb{X}_r = \{x \mid \|x\|^2 \leq r^2\} \subseteq \Omega$ should be designed based on Lemma 7 such that $\mathbb{X}_r \subseteq \Omega$ and $\kappa_f(\bar{p}_f^e)$ satisfies the tightened constraint (33c) for all $\bar{p}_f^e \in \mathbb{X}_r$.

Step 1: Determine the expression of set $\bar{\mathcal{U}}$ in (33c).

For the nonholonomic mobile robot with input constraint $\mathcal{U} = \{[v,\omega]^\top \mid \frac{|v|}{a} + \frac{|\omega|}{b} \leq 1\}$, the tightened constraint set $\bar{\mathcal{U}}$ can be described as $\bar{\mathcal{U}} = \{[v,\omega]^\top \mid \frac{|v|}{a} + \frac{|\omega|}{b} \leq q\}$, where constraint margin $q>0$ is determined by ϱ. As shown in Fig. 9, the blue area $\mathcal{U}$ is required to be tightened as the green area $\bar{\mathcal{U}}$, where $\hbar = \frac{\varrho}{sin(\vartheta)} = \frac{\varrho\sqrt{a^2+b^2}}{a}$. Therefore, the constraint margin q can be computed by $q = \frac{b-\hbar}{b} = 1 - \frac{\varrho\sqrt{a^2+b^2}}{ab}$.

Step 2: Determine the value of r such that $\kappa_f(\bar{p}_f^e)$ satisfies the tightened constraint (33c), i.e., $\kappa_f(\bar{p}_f^e) \in \bar{\mathcal{U}}$.

The terminal controller $\kappa_f(\bar{p}_f^e)$ can be abbreviated as

$$\kappa_f(\bar{p}_f^e) = \begin{bmatrix} \bar{\mu}_1\bar{x}_{f,1}^e + v_f^d \\ \frac{1}{\rho}\bar{\mu}_2\bar{x}_{f,2}^e + \omega_f^d \end{bmatrix} \triangleq \begin{bmatrix} v_f^\kappa \\ \omega_f^\kappa \end{bmatrix}$$

where $[v_f^d, \omega_f^d]^T$ is defined in Lemma 6 with $\frac{|v_f^d|}{a} + \frac{|\omega_f^d|}{b} \leq \gamma$. It holds that

$$\begin{aligned}
\frac{|v_f^\kappa|}{a} + \frac{|\omega_f^\kappa|}{b} &= \frac{|\bar{\mu}_1\bar{x}_{f,1}^e + v_f^d|}{a} + \frac{|\frac{1}{\rho}\bar{\mu}_2\bar{x}_{f,2}^e + \omega_f^d|}{b}\\
&\leq \frac{|v_f^d|}{a} + \frac{|\omega_f^d|}{b} + \frac{|\bar{\mu}_1\bar{x}_{f,1}^e|}{a} + \frac{|\bar{\mu}_2\bar{x}_{f,2}^e|}{a}\\
&\leq \gamma + \bar{\mu}_1\frac{|\bar{x}_{f,1}^e|}{a} + \bar{\mu}_2\frac{|\bar{x}_{f,2}^e|}{a}
\end{aligned}$$

with $b = a/\rho$. The constraint $\kappa_f(\bar{p}_f^e) \in \bar{\mathcal{U}}$ holds if $\bar{\mu}_1\frac{|\bar{x}_{f,1}^e|}{a} + \bar{\mu}_2\frac{|\bar{x}_{f,2}^e|}{a} \leq q-\gamma = 1 - \varrho\frac{\sqrt{(a^2+b^2)}}{ab} - \gamma$. In this sense, the parameter r can be chosen as $r = \frac{a}{\sqrt{\mu_1^2+\mu_2^2}}(1 - \varrho\frac{\sqrt{(a^2+b^2)}}{ab} - \gamma)$ being the maximal radius of the inscribed circle in set $\{\bar{p}_f^e \mid \bar{\mu}_1\frac{|\bar{x}_{f,1}^e|}{a} + \bar{\mu}_2\frac{|\bar{x}_{f,2}^e|}{a} \leq 1 - \varrho\frac{\sqrt{(a^2+b^2)}}{ab} - \gamma\}$.

(ii) Analogous to the analysis in (45), the feasible state $\tilde{p}_f^e(t_k+T|t_{k+1})$ lies in terminal region $\mathbb{X}_r$ and hereafter the controller switches to the terminal controller $\kappa_f(\cdot)$.

For $\tau\in[t_k+T, t_{k+1}+T)$, by using the terminal controller $\kappa_f(\cdot)$ and dynamic (30), we have

$$\begin{aligned}
&\dot{V}_f(\tilde{p}_f^e(\tau|t_{k+1})) = x_{f,1}^e\dot{x}_{f,1}^e + x_{f,2}^e\dot{x}_{f,2}^e\\
&= x_{f,1}^e(-v_f^\kappa + x_{f,2}^e\omega_f + (v_r - d_y\omega_r)\cos\theta_{rf} - d_x\omega_r\sin\theta_{rf})
\end{aligned}$$

$$+ x^e_{f,2}(-\rho\omega^\kappa_f - x^e_{f,1}\omega_f + (v_r - d_y\omega_r)\sin\theta_{rf} + d_x\omega_r\cos\theta_{rf})$$
$$= -\bar{\mu}_1 x^{e2}_{f,1} - \bar{\mu}_2 x^{e2}_{f,2} \le 2\bar{\mu}_{\min} V_f(\tilde{p}^e_f(\tau|t_{k+1})).$$

By the comparison principle, it holds that

$$V_f(\tilde{p}^e_f(\tau|t_{k+1})) \le V_f(\tilde{p}^e_f(t_k + T|t_{k+1}))e^{-2\bar{\mu}_{\min}(\tau - t_k - T)}$$

which implies

$$\|\tilde{p}^e_f(t_k + \delta + T|t_{k+1})\| \le \|\tilde{p}^e_f(t_k + T|t_{k+1})\|e^{-\bar{\mu}_{\min}\delta}.$$

Due to $\|\tilde{p}^e_f(t_k + T|t_{k+1})\| \le r$, the condition (ii) $\bar{\mu}_{\min}\delta \ge ln\frac{r}{\varepsilon}$ is derived to ensure

$$\|\tilde{p}^e_f(t_{k+1} + T|t_{k+1}))\| \le \varepsilon.$$

REFERENCES

[1] B. J. Rawlings and D. Q. Mayne. *Model Predictive Control: Theory and Design*. Madison, WI, USA: Nob Hill Pub, 2009.

[2] D. Q. Mayne, "Model predictive control: Recent developments and future promise," *Automatica*, vol. 50, no. 12, pp 2967–2986, 2014.

[3] P.O. M.Scokaert and D. Q. Mayne, "Min-max feedback model predictive control for constrained linear systems," *IEEE Trans. Autom. Control*, vol. 43, no. 8, pp 1136–1142, Aug. 1998.

[4] E. C. Kerrigan and J. M. Maciejowski, "Feedback min-max model predictive control using a single linear program: Robust stability and the explicit solution," *Int. J. Robust Nonlinear Control: IFAC-Affiliated J.*, vol. 14, no. 4, pp 395–413, 2004.

[5] D. Limón, T. Alamo, F. Salas, and E. F. Camacho, "On the stability of constrained MPC without terminal constraint," *IEEE Trans. Autom. Control*, vol. 51, no. 5, pp 832–836, May 2006.

[6] M. Lazar, D. M. D. L. Peña, W. P. M.H. Heemels, and T. Alamo, "On input-to-state stability of min-max nonlinear model predictive control," *Syst. Control Lett.*, vol. 57, no. 1, pp 39–48, 2008.

[7] D. P. Bertsekas and I. B. Rhodes, "On the minimax reachability of target sets and target tubes," *Automatica*, vol. 7, no. 2, pp 233–247, 1971.

[8] D. P. Bertsekas and I. B. Rhodes, "Recursive state estimation for a set-membership description of uncertainty," *IEEE Trans. Autom. Control*, vol. AC-16, no. 2, pp 117–128, Apr. 1971.

[9] D. Q. Mayne, M. M. Seron, and S. V. Raković, "Robust model predictive control of constrained linear systems with bounded disturbances," *Automatica*, vol. 41, no. 2, pp 219–224, 2005.

[10] Z. Peng and J. Wang, "Output-feedback path-following control of autonomous underwater vehicles based on an extended state observer and projection neural networks," *IEEE Trans. Syst. Man Cybern. Syst.*, vol. 48, no. 4, pp 535–544, Apr. 2018.

[11] J. Zhang, P. Shi, Y. Xia, and H. Yang, "Discrete-time sliding mode control with disturbance rejection," *IEEE Trans. Ind. Electron.*, vol. 66, no. 10, pp 7967–7975, Oct. 2019.

[12] Y. Li, M. Chen, L. Cai, and Q. Wu, "Resilient control based on disturbance observer for nonlinear singular stochastic hybrid system with partly unknown Markovian jump parameters," *J. Franklin Inst.*, vol. 355, no. 5, pp 2243–2265, 2018.

[13] J. Yang and W. X. Zheng, "Offset-free nonlinear MPC for mismatched disturbance attenuation with application to a static var compensator," *IEEE Trans. Circuits Syst. II: Exp. Briefs*, vol. 61, no. 1, pp 49–53, Jan. 2014.

[14] J. Yang, W. X. Zheng, S. Li, B. Wu, and M. Cheng, "Design of a prediction-accuracy-enhanced continuous-time MPC for disturbed systems via a disturbance observer," *IEEE Trans. Ind. Electron.*, vol. 62, no. 9, pp 5807–5816, Sep. 2015.

[15] J. Wang, F. Wang, Z. Zhang, S. Li, J. Rodriguez, and R. Kennel, "Design and implementation of disturbance compensation-based enhanced robust finite control set predictive torque control for induction motor systems," *IEEE Trans. Ind. Inform.*, vol. 13, no. 5, pp 2645–2656, Oct. 2017.

[16] H. T. Nguyen and J. Jung, "Disturbance rejection based model predictive control: Flexible-mode design with a modulator for three-phase inverters," *IEEE Trans. Ind. Electron.*, vol. 65, no. 4, pp 2893–2903, Apr. 2018.

[17] H. T. Nguyen, E. Kim, H. H. Choi, and J. Jung, "Model predictive control with modulated optimal vector for a three-phase inverter with an LC filter," *IEEE Trans. Power Electron.*, vol. 33, no. 3, pp 2690–2703, Mar. 2018.

[18] X. Zhang, B. Hou, and Y. Mei, "Deadbeat predictive current control of permanent-magnet synchronous motors with stator current and disturbance observer," *IEEE Trans. Power Electron.*, vol. 32, no. 5, pp 3818–3834, May 2017.

[19] U. Maeder, F. Borrelli, and M. Morari, "Linear offset-free model predictive control," *Automatica*, vol. 45, no. 10, pp 2214–2222, 2009.

[20] G. Pannocchia and A. Bemporad, "Combined design of disturbance model and observer for offset-free model predictive control," *IEEE Trans. Autom. Control*, vol. 52, no. 6, pp 1048–1053, Jun. 2007.

[21] U. Maeder and M. Morari, "Offset-free reference tracking with model predictive control," *Automatica*, vol. 46, no. 9, pp 1469–1476, 2010.

[22] M. Morari and U. Maeder, "Nonlinear offset-free model predictive control," *Automatica*, vol. 48, no. 9, pp 2059–2067, 2012.

[23] Z. Sun, Y. Xia, L. Dai, K. Liu, and D. Ma, "Disturbance rejection MPC for tracking of wheeled mobile robot," *IEEE/ASME Trans. Mechatronics*, vol. 22, no. 6, pp 2576–2587, Dec. 2017.

[24] Z. Liu, G. Lai, Y. Zhang, and C. L. P. Chen, "Adaptive fuzzy tracking control of nonlinear time-delay systems with dead-zone output mechanism based on a novel smooth model," *IEEE Trans. Fuzzy Syst.*, vol. 23, no. 6, pp. 1998–2011, Dec. 2015.

[25] F. A. Bayer, M. A. Muller, and F. Allgower, "Tube-based robust economic model predictive control," *J. Process Control*, vol. 24, no. 8, pp 1237–1246, 2014.

[26] Z. Sun, L. Dai, Y. Xia, and K. Liu, "Event-based model predictive tracking control of nonholonomic systems with coupled input constraint and bounded disturbances," *IEEE Trans. Autom. Control*, vol. 63, no. 2, pp 608–615, Feb. 2018.

[27] E. D. Sontag and Y. Wang, "New characterizations of input-to-state stability," *IEEE Trans. Autom. Control*, vol. 41, no. 9, pp 1283–1294, Sep. 1996.

[28] Z.- P. Jiang and Y. Wang, "Input-to-state stability for discrete-time nonlinear systems," *Automatica*, vol. 37, no. 6, pp 857–869, 2001.

[29] M. Rubagotti, D. M. Raimondo, A. Ferrara, and L. Magni, "Robust model predictive control with integral sliding mode in continuous-time sampled-data nonlinear systems," *IEEE Trans. Autom. Control*, vol. 56, no. 3, pp 556–570, Mar. 2011.

[30] C. V. Loan, "The sensitivity of the matrix exponential," *Siam J. Numer. Anal.*, vol. 14, no. 6, pp 971–981, 1977.

[31] L. Guo and W.-H. Chen, "Disturbance attenuation and rejection for systems with nonlinearity via DOBC approach," *Int. J. Robust Nonlinear Control: IFAC-Affiliated J.*, vol. 15, no. 3, pp 109–125, 2005.

[32] H. Xie, L. Dai, Y. Luo, and Y. Xia, "Robust MPC for disturbed nonlinear discrete-time systems via a composite self-triggered scheme," *Automatica*, vol. 127, 2021, Art. no. 109499, doi: 10.1016/j.automatica.2021.109499.

[33] H. Chen and F. Allgöwer, "A quasi-infinite horizon nonlinear model predictive control scheme with guaranteed stability," *Automatica*, vol. 34, no. 10, pp 1205–1217, 1998.

[34] M. Althoff, O. Stursberg, and M. Buss, "Reachability analysis of nonlinear systems with uncertain parameters using conservative linearization," in *Proc. Conf. Decis. Control*, 2008, pp. 4042–4048.

[35] Z. Sun and Y. Xia, "Receding horizon tracking control of unicycle-type robots based on virtual structure," *Int. J. Robust Nonlinear Control*, vol. 26, no. 17, pp 3900–3918, 2016.

[36] S. Yu, C. Maier, H. Chen, and F. Allgöwer, "Tube MPC scheme based on robust control invariant set with application to Lipschitz nonlinear systems," *Syst. Control Lett.*, vol. 62, no. 2, pp 194–200, 2013.

[37] M. Farina and R. Scattolini, "Tube-based robust sampled-data MPC for linear continuous-time systems," *Automatica*, vol. 48, no. 7, pp 1473–1476, 2012.

[38] Y. Chen, Z. Li, H. Kong, and F. Ke, "Model predictive tracking control of nonholonomic mobile robots with coupled input constraints and unknown dynamics," *IEEE Trans. Ind. Inform.*, vol. 15, no. 6, pp. 3196–3205, Jun. 2019.

[39] M. Rubagotti, A. Estrada, F. Castanos, A. Ferrara, and L. Fridman, "Integral sliding mode control for nonlinear systems with matched and unmatched perturbations," *IEEE Trans. Autom. Control*, vol. 56, no. 11, pp. 2699–2704, Nov. 2011.

[40] J. Zhang, X. Liu, Y. Xia, Z. Zuo, and Y. Wang, "Disturbance observer-based integral sliding-mode control for systems with mismatched disturbances," *IEEE Trans. Ind. Electron.*, vol. 63, no. 11, pp. 7040–7048, Nov. 2016.

[41] T. Hastie, J. Friedman, and R. Tibshirani, *The Elements of Statistical Learning: Data Mining, Inference, and Prediction*. New York, NY, USA: Springer, 2008.

[42] Y. M. Nechepurenko, "Bounds for the matrix exponential based on the Lyapunov equation and limits of the Hausdorff set," *Comput. Math. Math. Phys.*, vol. 42, no. 2, pp. 125–134, 2002.

[43] K. HassanKhalil. *Nonlinear Systems*. Upper Saddle River, NJ, USA: Prentice-Hall, 2002.
[44] H. Li and Y. Shi, "Network-based predictive control for constrained nonlinear systems with two-channel packet dropouts," *IEEE Trans. Ind. Electron.*, vol. 61, no. 3, pp. 1574–1582, Mar. 2014.
[45] Z. Sun, L. Dai, K. Liu, D. V. Dimarogonas, and Y. Xia, "Robust self-triggered MPC with adaptive prediction horizon for perturbed nonlinear systems," *IEEE Trans. Autom. Control*, vol. 64, no. 11, pp 4780–4787, Nov. 2019.
[46] D. Limón, T. Alamo, F. Salas, and E. F. Camacho, "Input to state stability of min-max MPC controllers for nonlinear systems with bounded uncertainties," *Automatica*, vol. 42, no. 5, pp 797–803, 2006.
[47] G. Pin, D. M. Raimondo, L. Magni, and T. Parisini, "Robust model predictive control of nonlinear systems with bounded and state-dependent uncertainties," *IEEE Trans. Autom. Control*, vol. 54, no. 7, pp 1681–1687, Jul. 2009.
[48] S. El-Ferik, A. B.Siddiqui, and F. L. Lewis, "Distributed nonlinear MPC of multi-agent systems with data compression and random delays," *IEEE Trans. Autom. Control*, vol. 61, no. 3, pp 817–822, Mar. 2016.
[49] M. Lazar and W. P. M.H. Heemels, "Predictive control of hybrid systems: Input-to-state stability results for sub-optimal solutions," *Automatica*, vol. 45, no. 1, pp 180–185, 2009.
[50] G. C. Konstantopoulos, Q.-C. Zhong, B. Ren, and M. Krstic, "Bounded integral control of input-to-state practically stable nonlinear systems to guarantee closed-loop stability," *IEEE Trans. Autom. Control*, vol. 61, no. 12, pp 4196–4202, Dec. 2016.

Huahui Xie received the B.S. degree in electrical engineering and automation in 2018 from the Beijing Institute of Technology, Beijing, China, where he is currently working toward the Ph.D. degree in control science and engineering.

His research interests include event-triggered control and model predictive control.

Li Dai received the B.S. degree in information and computing science and the Ph.D. degree in control science and engineering from the Beijing Institute of Technology, Beijing, China, in 2010 and 2016, respectively.

Dr. Dai is currently an Associate Professor with the School of Automation, Beijing Institute of Technology. Her research interests include model predictive control, distributed control, data-driven control, stochastic systems, and networked control systems.

Yuchen Lu was born in Xining, Qinghai Province, China, in 1996. He received the B.S. degree in automation from the School of Automation, Beijing Institute of Technology, Beijing, China, in 2018.

His research interests include model predictive control and wheeled mobile robots.

Yuanqing Xia (Senior Member, IEEE) received the Ph.D. degree in control theory and control engineering from Beihang University, Beijing, China, in 2001.

He was a research fellow in several academic institutions from 2002 to 2008, including the National University of Singapore, Singapore, and the University of Glamorgan, Pontypridd, U.K. Since 2004, he has been with the Beijing Institute of Technology (BIT), Beijing, China, where he is currently a Chair Professor, as well as the Chief Director of the School of Automation. He has authored or coauthored 16 monographs in Springer, John Wiley, and CRC, and more than 400 papers in international scientific journals, and has been a highly cited scholar since 2014 by Elsevier. His research interests include cloud control systems, networked control systems, robust control and signal processing, active disturbance rejection control, unmanned system control, and flight control.

Dr. Xia is currently the Director of specialized committee on cloud control and decision of Chinese Institute of Command and Control (CICC), a Member of the 8th Disciplinary Review Group of the Academic Degrees Committee of the State Council, a Member of the Big Data Expert Committee of the Chinese Computer Society, and the Vice Chairman of the Internet of Things Working Committee of the Chinese Institute of Instrumentation. He was granted by the National Outstanding Youth Foundation of China in 2012, and was honored as the Yangtze River Scholar Distinguished Professor in 2016 and the Leading Talent of the Chinese Ten Thousand Talents Program. He is the Deputy Editor of the *Journal of Beijing Institute of Technology*, an Associate Editor of *Acta Automatica Sinica*, *International Journal of Automation and Computing*, *Gyroscopy and Navigation*, *Control Theory and Applications*, etc. He obtained the Second Award of the Beijing Municipal Science and Technology (No. 1) in 2010 and 2015, the Second National Award for Science and Technology (No. 2) in 2011, the Second Natural Science Award of the Ministry of Education (No. 1) in 2012 and 2017, and the Second Wu Wenjun Artificial Intelligence Award in 2018 (No. 1). More than five of his students have obtained the excellent doctoral thesis awards from the Chinese Association of Automation or Chinese Institute of Command and Control.